Artemisia pollen dataset for exploring the potential ecological indicators in deep time

Li-Li Lu[a,d†], Bo-Han Jiao [a,d†], Feng Qin [b†], Gan Xie[a†], Kai-Qing Lu[a,d], Jin-Feng Li[a], Bin Sun[a], Min Li[a],

David K. Ferguson[c], Tian-Gang Gao[a,d *], Yi-Feng Yao[a,d*], Yu-Fei Wang[a,d*]

[a]*State Key Laboratory of Systematic and Evolutionary Botany, Institute of Botany, Chinese Academy of*

Sciences, 20 Nanxincun Xiangshan, Beijing 100093, China

[b]*Key Laboratory of Land Surface Pattern and Simulation, Institute of Geographic Sciences and Natural*

Resources Research, Chinese Academy of Sciences, Beijing 100101, China

[c]*Department of Paleontology, University of Vienna, Althanstrasse 14, Vienna A-1090, Austria*

[d]*University of Chinese Academy of Sciences, Beijing 100049, China*

[†] These authors contributed equally to this work.

[*]Corresponding authors. Tel: +86 (10) 62836439.

Email addresses: gaotg@ibcas.ac.cn (T. G. GAO); yaoyf@ibcas.ac.cn (Y. F. YAO); wangyf@ibcas.ac.cn (Y.

F. WANG).

Abstract. *Artemisia*, along with Chenopodiaceae is the dominant component growing in the desert and dry grassland of the Northern Hemisphere. *Artemisia* pollen with its high productivity, wide distribution, and easy identification, is usually regarded as an eco-indicator for assessing aridity and distinguishing grassland from desert vegetation in terms of the pollen relative abundance ratio of Chenopodiaceae/*Artemisia* (C/A). Nevertheless, divergent opinions on the degree of aridity evaluated by *Artemisia* pollen have been circulating in the palynological community for a long time. To solve the confusion, we first selected 36 species from 9 clades and 3 outgroups of *Artemisia* based on the phylogenetic framework, which attempts to cover the maximum range of pollen morphological variation. Then, sampling, experiments, photography, and measurements were taken using standard methods. Here, we present pollen datasets containing 4018 original pollen photographs, 9360 pollen morphological trait measurements~~statistical pollen morphological traits~~, information on 30858 source plant occurrences, and corresponding environmental factors. Hierarchical cluster analysis on pollen morphological traits was carried out to subdivide *Artemisia* pollen into three types. When plotting the three pollen types of *Artemisia* onto the global terrestrial biomes, different pollen types of *Artemisia* were found to have different habitat ranges. These findings change the traditional concept of *Artemisia* being restricted to arid and semi-arid environments. The data framework that we designed is open and expandable for new pollen data of *Artemisia* worldwide. In the future, linking pollen morphology with habitat via these pollen datasets will create additional knowledge that will increase the resolution of the ecological environment in the geological past. The *Artemisia* pollen datasets are freely available at Zenodo (https://doi.org/10.5281/zenodo.6900308~~6791891~~; Lu et al., 2022).

1 Introduction

The concept of global change can be considered as any consistent trend in the environment - past, present, or projected - that affects a substantial part of the globe. Consequently past climates shed light on our future (Tierney et al., 2020). When attempting to reconstruct past global change prior to meteorological records, we need some appropriate biological or abiotic proxies based on long-term, consistently collected data, e.g. leaf wax biomarkers (Bhattacharya et al., 2018), tree-ring data (Moberg et al., 2005), leaf form (Yang et al., 2015), pollen data (Mosbrugger et al., 2005; Guiot and Cramer, 2016; Marsicek et al., 2018), atmospheric carbon dioxide (Zachos et al., 2008; Beerling and Royer, 2011), and isotope records (Zachos et al., 2001; Sánchez-Murillo et al., 2019). Determining a suitable proxy to reconstruct palaeoclimate and palaeoenvironment is a great scientific challenge (Tierney et al., 2020; McClelland et al., 2021).

The pollen of *Artemisia* (A), together with that of Chenopodiaceae (C) in arid and semi-arid areas, in the form of the ratio of C/A pollen abundance, was applied to distinguish grassland and desert vegetation types and assess the degree of drought in the geological past (El-Moslimany, 1990; Sun et al., 1994; Davies and Fall, 2001; Herzschuh et al., 2004; Xu et al., 2007; Zhao et al., 2009; Zhang et al., 2010; Zhao et al., 2012; Li et al., 2017; Ma et al., 2017; Koutsodendris et al., 2019; Wang et al., 2020), because both Chenopodiaceae and *Artemisia* are dominant elements of desert vegetation (China Vegetation Editorial Committee, 1980; Vrba, 1980; Tarasov et al., 1998; Herzschuh et al., 2004; Li et al., 2010; Zhao et al., 2021), and the sum of their pollen relative abundances in the surface soil is usually more than 50% in arid and semi-arid areas (Sun et al., 1994; Lu et al., 2020).

Among them, the pollen of *Artemisia*, with its high productivity, wide spatial and temporal distribution, easy identification, and morphological uniformity under the light microscope (LM), is an essential component and useful bio-indicator in pollen-based past vegetation reconstructions and environmental assessments. Some researchers regarded *Artemisia* as an aridity indicator (El-Moslimany, 1990; Yi et al., 2003a; Yi et al., 2003b; Liu et al., 2006; Cai et al., 2019; Cui et al., 2019; Chen et al., 2020; Wu et al., 2020; Cao et al., 2021), while others suggested that the correlation between the relative abundance of *Artemisia* pollen and humidity was insignificant (Weng et al., 1993; Sun et al., 1996; Koutsodendris et al., 2019; Lu et al., 2020; Zhao et al., 2021). Consequently, there is an urgent need to evaluate whether different pollen types of *Artemisia* represent distinct habitats.

In the past, *Artemisia* pollen was regarded as very uniform under LM (Wodehouse, 1926; Sing and Joshi, 1969; Ling, 1982; Wang et al., 1995). For instance, following the description and statistics of pollen morphology of 27 species of *Artemisia* in Eurasia under LM, Sing and Joshi (1969) stated that the pollen grains of *Artemisia* are consistent and continuous in morphology. Later, some authors recognized a series of pollen types (Chen, 1987; Jiang et al., 2005; Ghahraman et al., 2007; Shan et al., 2007; Hayat et al., 2009; Hayat et al., 2010; Hussain et al., 2019), based on a detailed survey of the pollen micromorphology of different taxa under the scanning electron microscope (SEM).

For example, Chen (1987) described the pollen morphology of 77 *Artemisia* species from China under LM and SEM and divided these pollen grains into six types by using pollen characters, such as the shape and size of the spinules as well as the density of spinules and granules. Type I (sparse spinules with granules among them), type II (dense spinules, no or few granules), type III (sparse spinules, no granules), type IV (dense spinules, well-developed granules), type V (small and sparse spinules, smooth tectum) and type VI (dissimilar spinules with granules among them).

Shan et al. (2007) investigated the pollen morphology of 32 *Artemisia* species from the Loess Plateau of China under LM and SEM and divided these pollen grains into five types according to exine sculpture: type I (dense spinules with swollen bases, small granules), type II (dense spinules, swollen bases almost united), type III (dense spinules with swollen bases and smooth tectum), type IV (sparse small spinules and smooth tectum) and type V (sparse spinules, small granules).

Jiang et al. (2005) observed the pollen morphology of 57 representative plants in 7 groups of *Artemisia* under LM and SEM. This pollen can be divided into two types based on exine sculpture: type I (spinules multi-ruminated with flared bases, connecting the mostly densely arranged spinules) and type II (densely or loosely arranged spinules without flared bases, interspace glandular or smooth) with subtypes II-1, II-2, II-3, and II-4 based on the distribution of the spinules.

Ghahraman et al. (2007) studied the pollen morphology of 26 species of the 33 *Artemisia* species in Iran under LM and SEM. Based on exine ornamentation observed under SEM, two types of pollen grains were recognized: type I, exine surface covered with dense acute spinules, and type II, exine surface with few spinules.

Hayat et al. (2009, 2010) carried out a palynological study of 22 *Artemisia* species from Pakistan under LM and SEM. Earlier work demonstrated the phylogenetic associations within *Artemisia* based on a phylogenetic analysis of 9 characters (pollen type, pollen shape, spinule arrangement, exine sculpture, spinule

92 base, the length of polar axis, the length of equatorial axis, exine thickness, and colpus width) of pollen grains

93 of *Artemisia*. In the latter work, eight micromorphological characters were identified and pooled by cluster

94 analysis, leading to the recognition of 5 groups.

95 Hussain et al. (2019) studied the pollen morphology of 15 *Artemisia* species in the Gilgit-Baltistan region

96 of Pakistan utilizing SEM and divided these species into four groups based on cluster analysis of seven

97 micromorphological characters (pollen type, pollen shape, spinule arrangement, exine sculpture, spinule base,

98 polar length, and equatorial width).

99 Almost all of the above-mentioned *Artemisia* pollen classifications were designed to solve taxonomic or

100 phylogenetic problems, and only a few were concerned with linking diverse habitats to the different pollen

101 types in *Artemisia*.

102 Here we attempt to 1) present abundant pollen photographs of 36 species from 9 branches and 3

103 outgroups of the genus (ca. 400 species worldwide, see Ling, 1982; Bremer and Humphries, 1993),

104 constrained by the phylogenetic framework of *Artemisia* (Sanz et al., 2008; Malik et al., 2017); 2) describe

105 and measure the morphological traits of these pollen grains; 3) provide a new classification of pollen types

106 and their distribution worldwide, with a key to pollen types in *Artemisia*; 4) explore the diverse ecological

107 niches of *Artemisia* represented by different pollen types in order to evaluate palaeovegetation and reconstruct

108 palaeoenvironments.

109 **2 Materials and methods**

110 **2.1 Sampling strategy**

111 The 36 pollen samples studied were selected from voucher sheets in the PE herbarium at the Institute of

112 Botany, Chinese Academy of Sciences (Fig. 1, Table B1), covering 9 main clades, i.e., Subg. *Tridentata*, Subg.

113 *Artemisia* (contains Sect. *Artemisia*, Sect. *Abrotanum* I, Sect. *Abrotanum* II and Sect. *Abrotanum* III), Subg.

114 *Pacifica*, Subg. *Seriphidium*, Subg. *Absinthium*, and Subg. *Dracunculus*, constrained by the phylogenetic

115 framework of *Artemisia* (Malik et al., 2017) and 3 outgroups (Sanz et al., 2008), reflecting the maximum

116 diversity or morphological variation under LM and SEM.

117

Figure 1. Phylogenetic tree of *Artemisia* (modified from Malik et al., 2017). The styles of the strokes that were used to draw the branches indicate the traditional subgeneric classification of *Artemisia*, and the yellow spots indicate sampled taxa.

2.2 Data acquisition

Pollen samples were acetylized by the standard method (Erdtman, 1960) and fixed in glycerine jelly. Standard procedures were followed for LM and SEM (Chen, 1987; Wang et al., 1995). The pollen grains were photographed under LM (Leica DM 4000) at a magnification of ×1000 and SEM (Hitachi S-4800) at an accelerating voltage of 30 kV. The pollen terminology followed the descriptions of Hesse et al. (2009) and

Halbritter et al. (2018). The statistical pollen morphological traits under LM (Figs. 2a-b, P: Polar length; E: Equatorial width; P/E; T: Exine thickness; L: Pollen length; T/L) of each species were measured using 20 pollen grains. We chose five pollen grains under SEM for each exine ornamentation trait in each species (Figs. 2c-f, D: Diameter of spinule base; H: Spinule height; D/H; Gs: Granule spacing; Ss: Spinule spacing; Gs/Ss; Ps: Perforation spacing), and on average, randomly selected four regions of each pollen grain for measuring, yielding a total of 20 measurements. The mean value (M) and standard deviation (SD) of the pollen grains of each species were measured and calculated in both polar and equatorial views (Appendix A, Table 1).
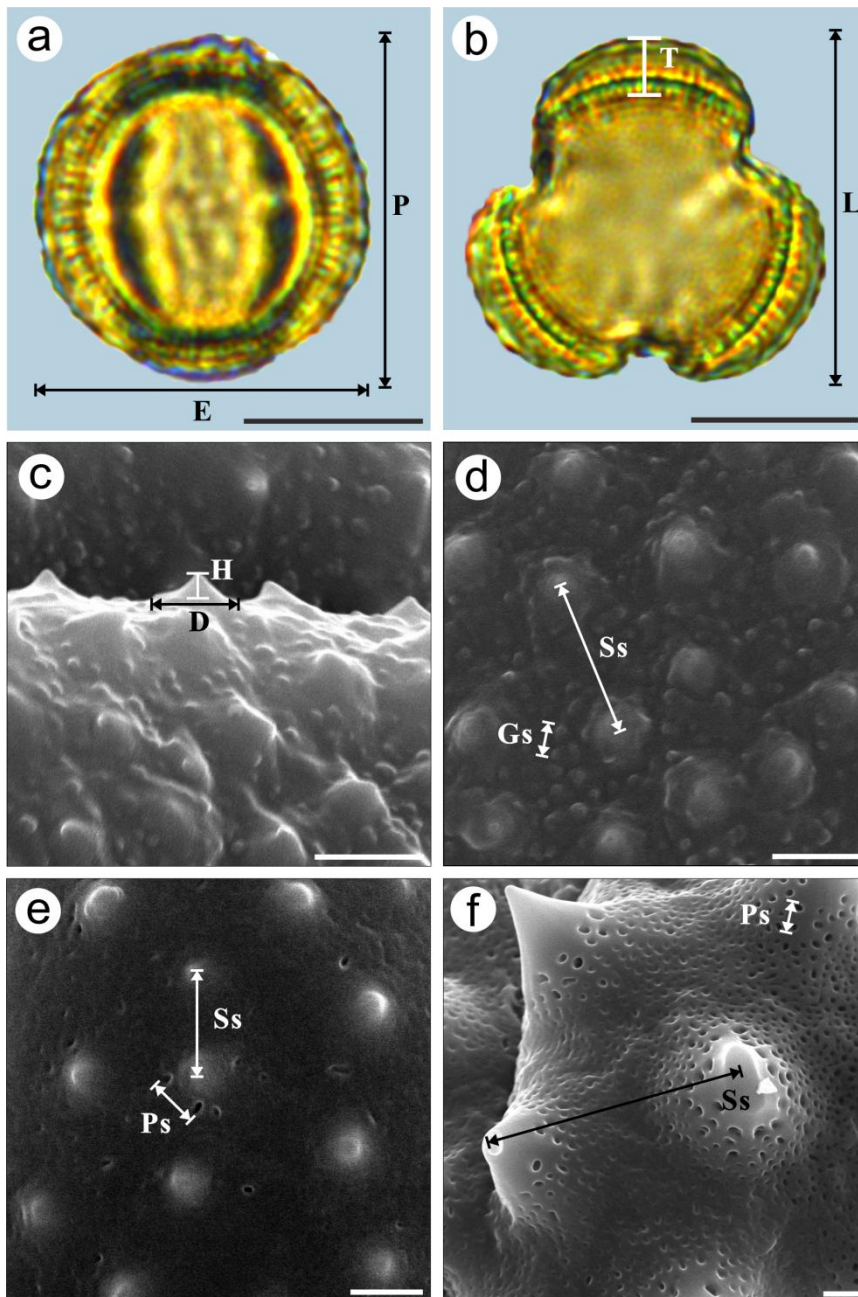
Figure 2. Graphical illustration of measured pollen morphological traits in *Artemisia (*a-b: *A. annua*; c-d: *A. vulgaris)* and outgroups (e: *Kaschagaria brachanthemoides;* f: *Ajania pallasiana*). Scale bar in LM and SEM overview 10 μm, in SEM close-up 1 μm.

The scientific names of selected taxa were standardized according to Plants of the World Online (https://powo.science.kew.org/). The specimen sampling coordinates of the corresponding taxa were obtained from the Global Biodiversity Information Facility (GBIF, https://www.gbif.org/). Only preserved specimens were filtered for GBIF data given their well-documented geographical information and the availability of specimens as definitive vouchers. The distribution data on observations and cultivated collections provided by GBIF were excluded because they may contain incorrect identification or incorrect geo-referencing (Brummitt et al., 2020). Next, the distribution data was standardized cleaned using R package "CoordinateCleaner" (Zizka et al., 2019); no outliers were found.

The corresponding environmental factors including altitude and 19 climate parameters of these coordinates were obtained from WorldClim (https://www.worldclim.org/) with a spatial resolution of 30 seconds (~1 km^2) in 1970-2000 by Extract MultiValues To Points using ArcGIS 10.2 software in bilinear interpolation.

2.3 Data processing

OriginPro 2021 software was used for hierarchical cluster analysis on *Artemisia* and its outgroup pollen data. The Euclidean distance was calculated after the normalization of the original data, and the Ward method was used for clustering. Five groups were established, and the center point of each group was calculated according to the sum of distances. Pollen morphological traits for the principal component analysis (PCA) of *Artemisia* and its outgroups and grouped according to the five groups of the cluster analysis. OriginPro 2021 software was used to draw group violin diagrams and boxplots respectively, and run an ANOVA to test for an overall difference between the pollen characters of 3 pollen types and testing intraspecific variability in pollen exine ultrastructure characters among three representative species, followed by post hoc tests (Tukey). OriginPro 2021 software was also used to run correlation coefficients analysed by the Pearson correlation between pollen morphological traits and environmental factors as well as draw group violin diagrams and run a KWANOVA to test for overall differences between the environmental factors of the 3 pollen types. The images of habitats reproduced in the text are from the websites listed in Table B1.

162   The global distribution data of the 36 representative species and 3 pollen types were plotted on the map

163   of terrestrial ecological regions (Olson et al., 2001) using ArcGIS 10.2 software (Figs. 16, 2~~0~~1).

164   **3 Data description**

165   **3.1 *Artemisia* pollen grains and their source plant habitats**

166   Here we provide detailed data on pollen morphological traits, covering 36 species from 9 main clades of

167   *Artemisia* and 3 outgroups constrained by the phylogenetic framework (Fig. 1, Sanz et al., 2008; Malik et al.,

168   2017) under LM and SEM, the habitats of their source plants (Figs. 3-14).

169
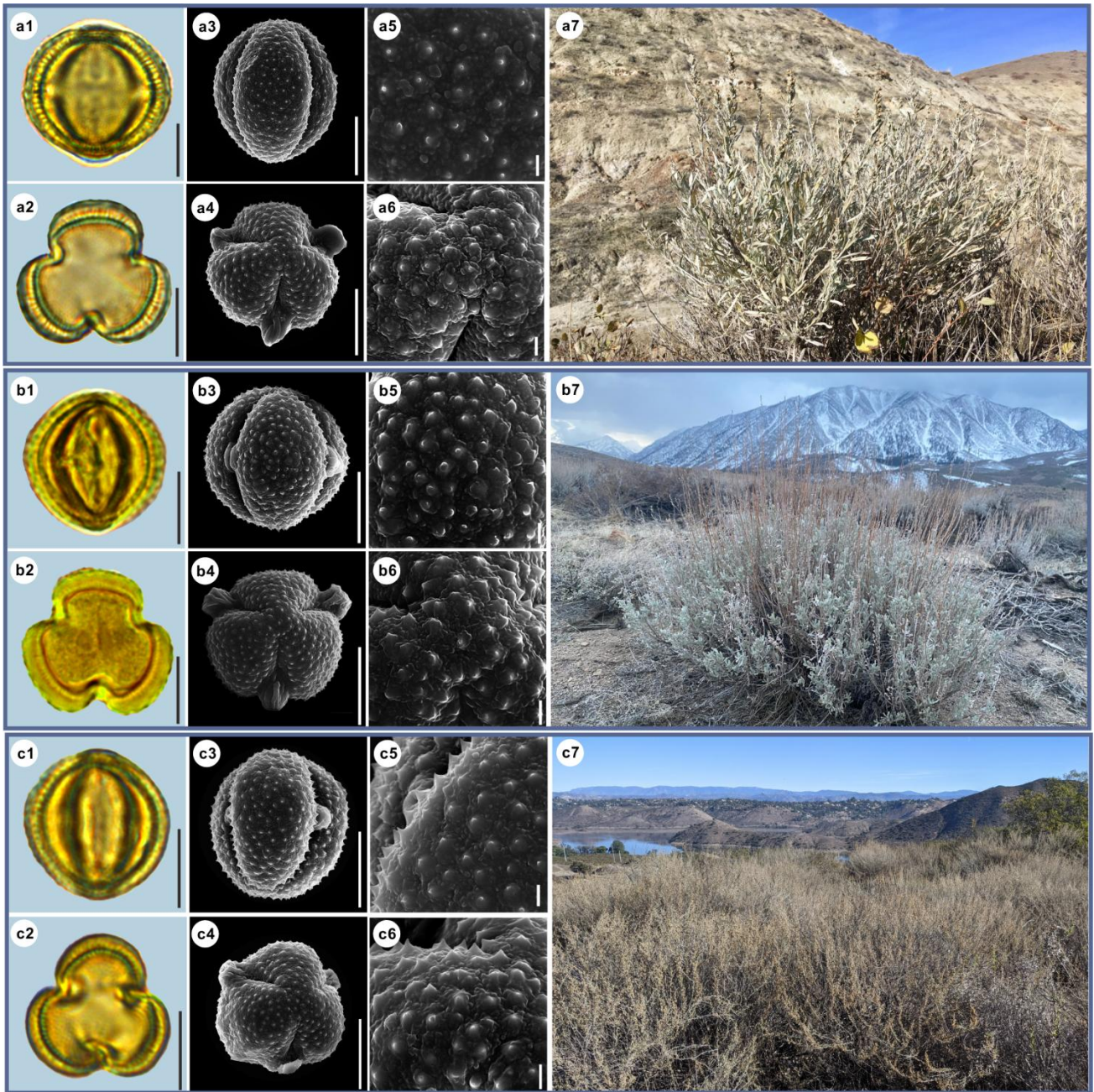
Figure 3. Pollen grains and the habitats of their source plants.

a. *Artemisia cana*; b. *Artemisia tridentata*; c. *Artemisia californica*.

Pollen grains in equatorial view under LM (a1, b1, c1) and SEM (a3, a5, b3, b5, c3, c5), in polar view under LM (a2, b2, c2) and SEM (a4, a6, b4, b6, c4, c6), along with the habitats of their source plants (a7 cited from https://www.inaturalist.org/photos/54492753 by © Jason Headley, b7 cited from https://www.inaturalist.org/photos/117436654 by © Matt Berger, c7 cited from https://www.inaturalist.org/photos/108921528 by © Don Rideout).

Scale bar in LM and SEM overview 10 μm, in SEM close-up 1 μm.

178
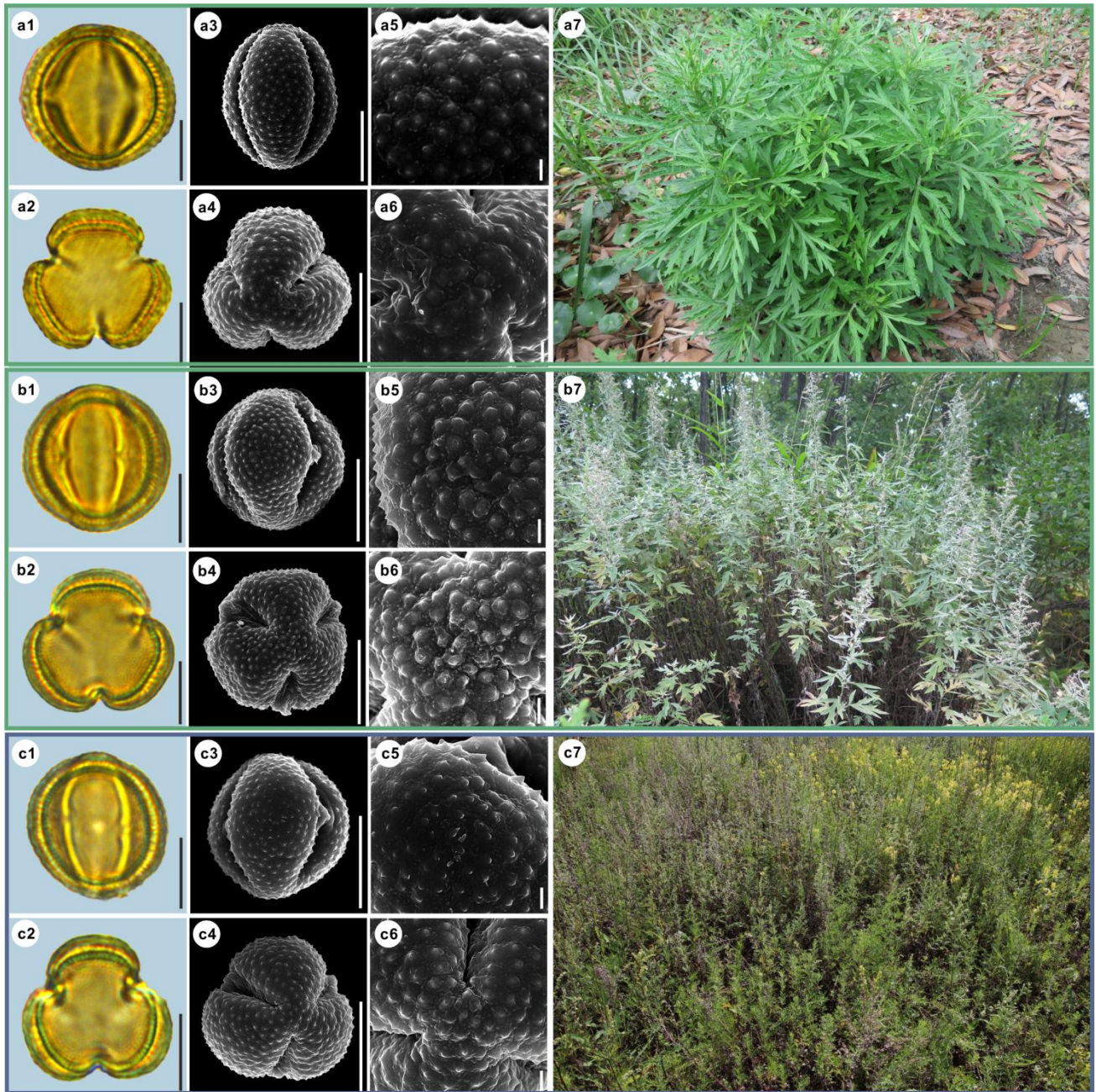
Figure 4. Pollen grains and the habitats of their source plants.

a. *Artemisia indica*; b. *Artemisia argyi*; c. *Artemisia mongolica*.

Pollen grains in equatorial view under LM (a1, b1, c1) and SEM (a3, a5, b3, b5, c3, c5), in polar view under LM (a2, b2, c2) and SEM (a4, a6, b4, b6, c4, c6), along with the habitats of their source plants (a7 cited from https://www.inaturalist.org/photos/66336449 by © yangting, b7 cited from https://www.inaturalist.org/photos/95820686 by © sergeyprokopenko, c7 cited from https://www.inaturalist.org/photos/163584035 by © Nikolay V Dorofeev).

Scale bar in LM and SEM overview 10 μm, in SEM close-up 1 μm.

187
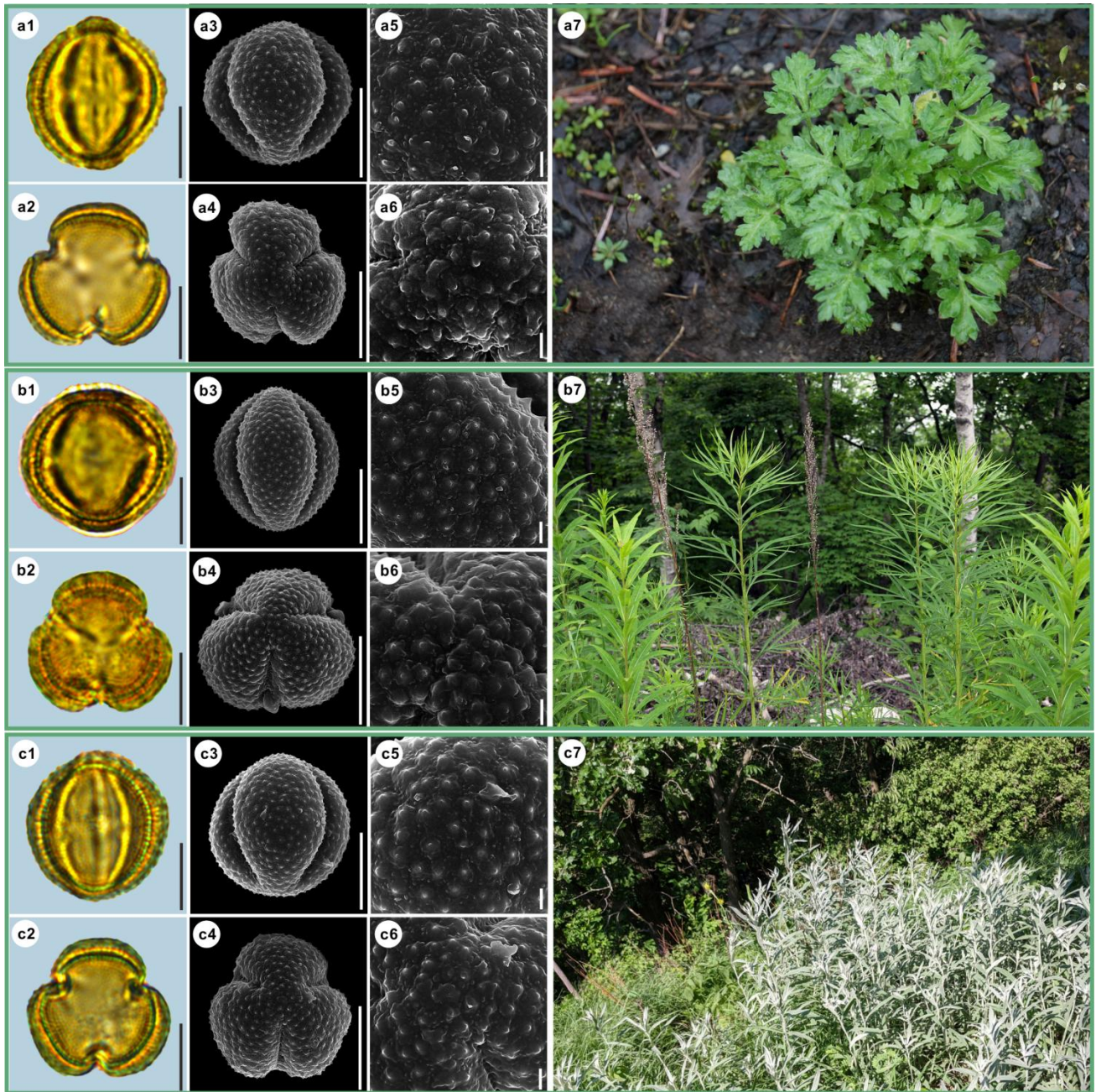
Figure 5. Pollen grains and the habitats of their source plants.

a. *Artemisia vulgaris*; b. *Artemisia selengensis*; c. *Artemisia ludoviciana*.

Pollen grains in equatorial view under LM (a1, b1, c1) and SEM (a3, a5, b3, b5, c3, c5), in polar view under LM (a2, b2, c2) and SEM (a4, a6, b4, b6, c4, c6), along with the habitats of their source plants (a7 cited from https://www.inaturalist.org/photos/120600448 by © Sara Rall, b7 cited from https://www.inaturalist.org/photos/46352423 by © Gularjanz Grigoryi Mihajlovich, c7 cited from https://www.inaturalist.org/photos/77690333 by © Ethan Rose).

Scale bar in LM and SEM overview 10 μm, in SEM close-up 1 μm.

196
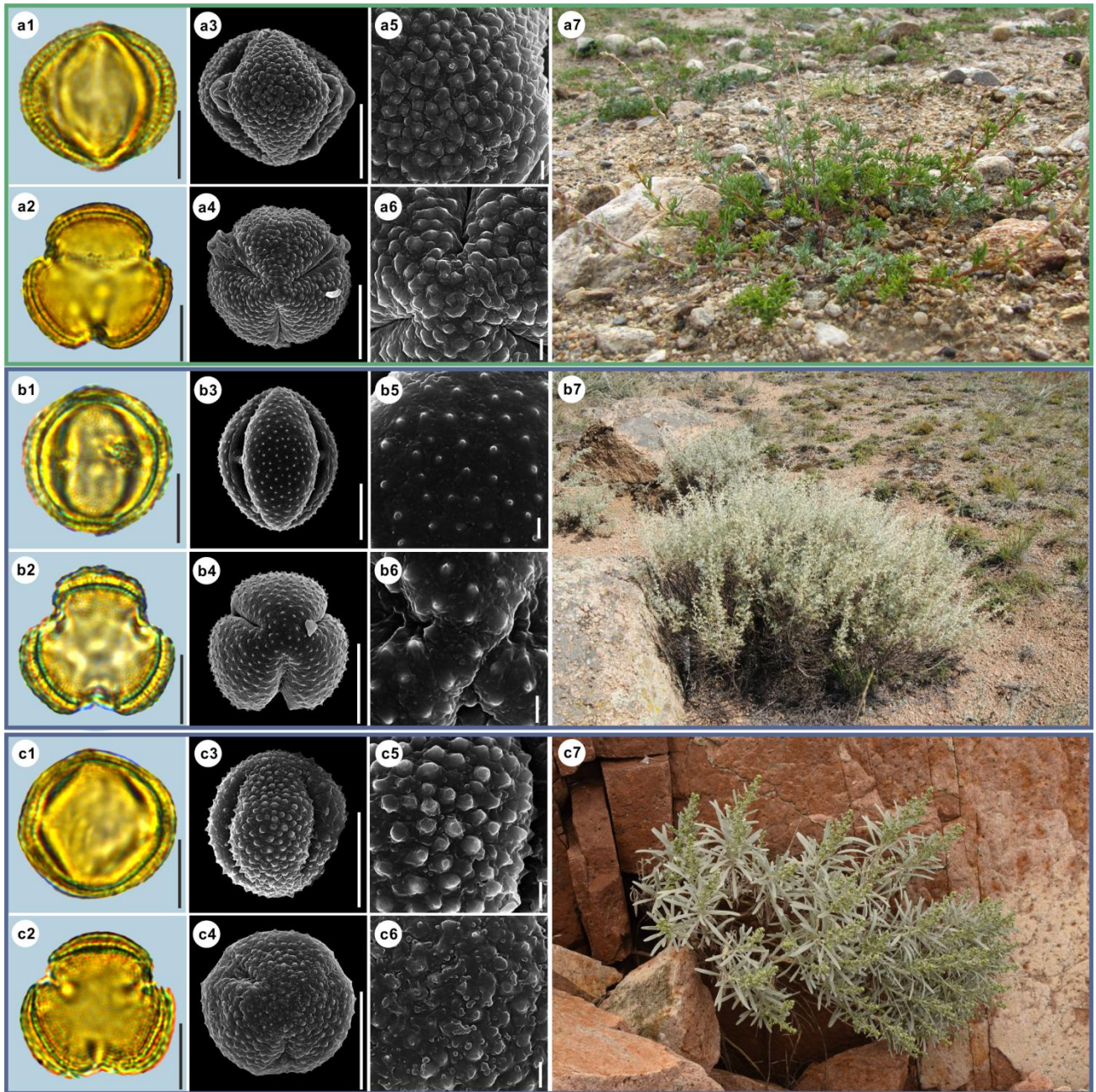
Figure 6. Pollen grains and the habitats of their source plants.

a. *Artemisia roxburghiana*; b. *Artemisia rutifolia*; c. *Artemisia chinensis*.

Pollen grains in equatorial view under LM (a1, b1, c1) and SEM (a3, a5, b3, b5, c3, c5), in polar view under LM (a2, b2, c2) and SEM (a4, a6, b4, b6, c4, c6), along with the habitats of their source plants (a7 provided by © Bo-Han Jiao, b7 cited from https://www.inaturalist.org/photos/62207191 by © Daba, c7 provided by © Jia-Hao Shen).

Scale bar in LM and SEM overview 10 μm, in SEM close-up 1 μm.
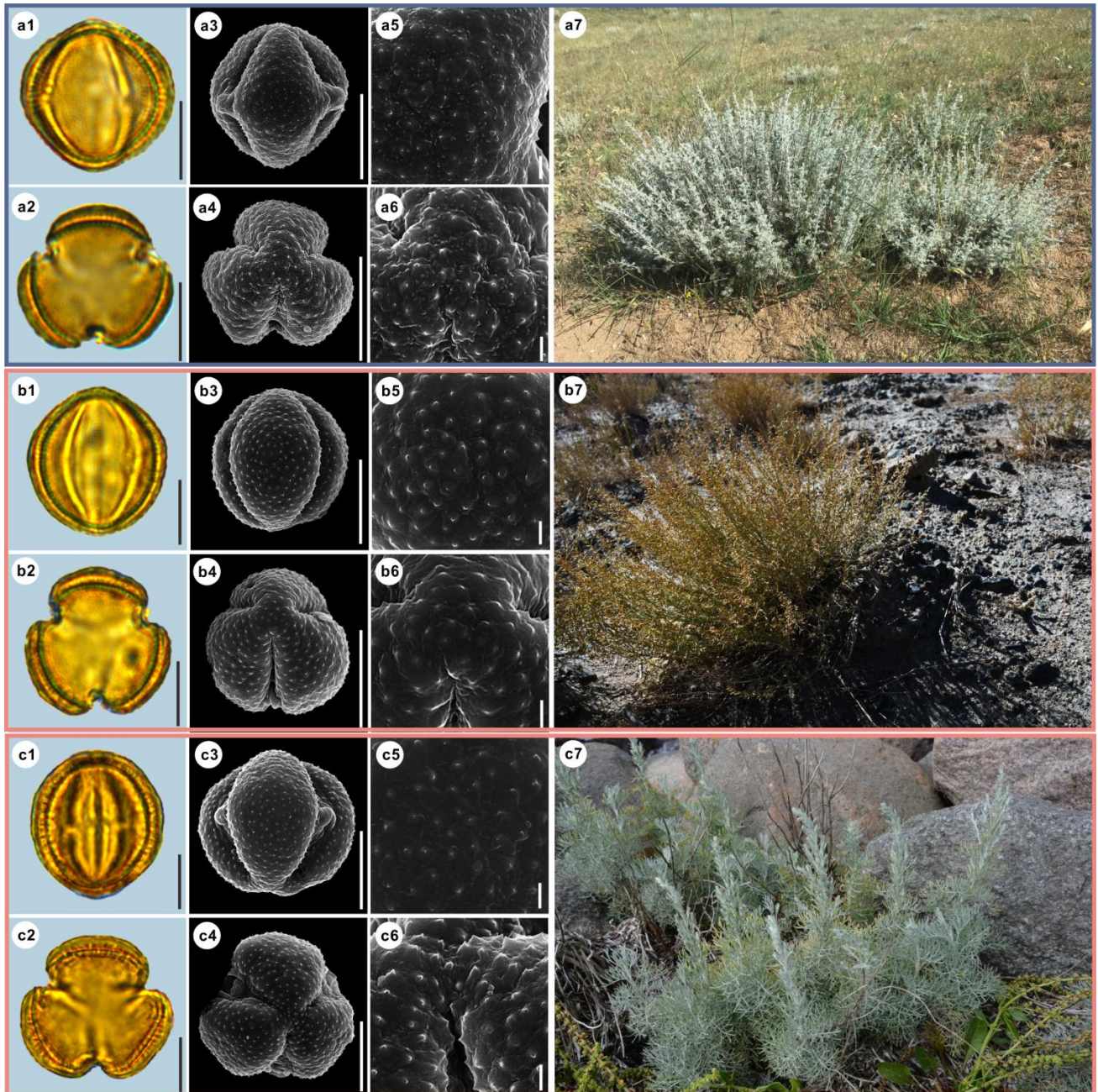
Figure 7. Pollen grains and the habitats of their source plants.

a. *Artemisia kurramensis*; b. *Artemisia compactum*; c. *Artemisia maritima*.

Pollen grains in equatorial view under LM (a1, b1, c1) and SEM (a3, a5, b3, b5, c3, c5), in polar view under LM (a2, b2, c2) and SEM (a4, a6, b4, b6, c4, c6), along with the habitats of their source plants (a7 cited from https://www.inaturalist.org/photos/133758174 by © Andrey Vlasenko, b7 provided by © Chen Chen, c7 cited from https://www.inaturalist.org/photos/86515371 by © torkild).

Scale bar in LM and SEM overview 10 μm, in SEM close-up 1 μm.

212
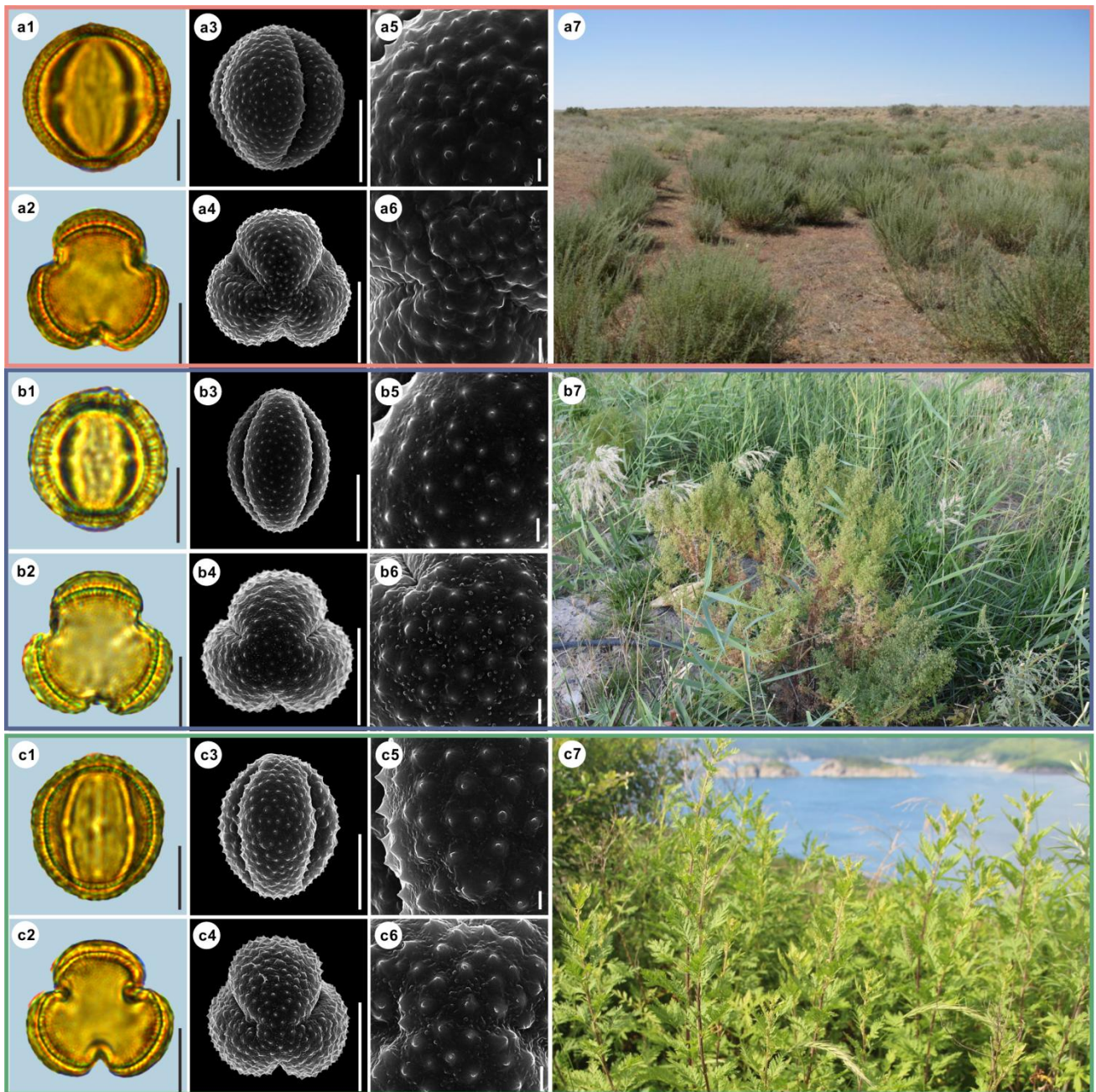
Figure 8. Pollen grains and the habitats of their source plants.

a. *Artemisia aralensis*; b. *Artemisia annua*; c. *Artemisia freyniana*.

Pollen grains in equatorial view under LM (a1, b1, c1) and SEM (a3, a5, b3, b5, c3, c5), in polar view under LM (a2, b2, c2) and SEM (a4, a6, b4, b6, c4, c6), along with the habitats of their source plants (a7 cited from https://www.plantarium.ru/lang/en/page/image/id/73063.html by © Полынь аральская, b7 provided by © Chen Chen, c7 cited from https://www.inaturalist.org/photos/154390279 by © Шильников Дмитрий Сергеевич).

Scale bar in LM and SEM overview 10 µm, in SEM close-up 1 µm.

221
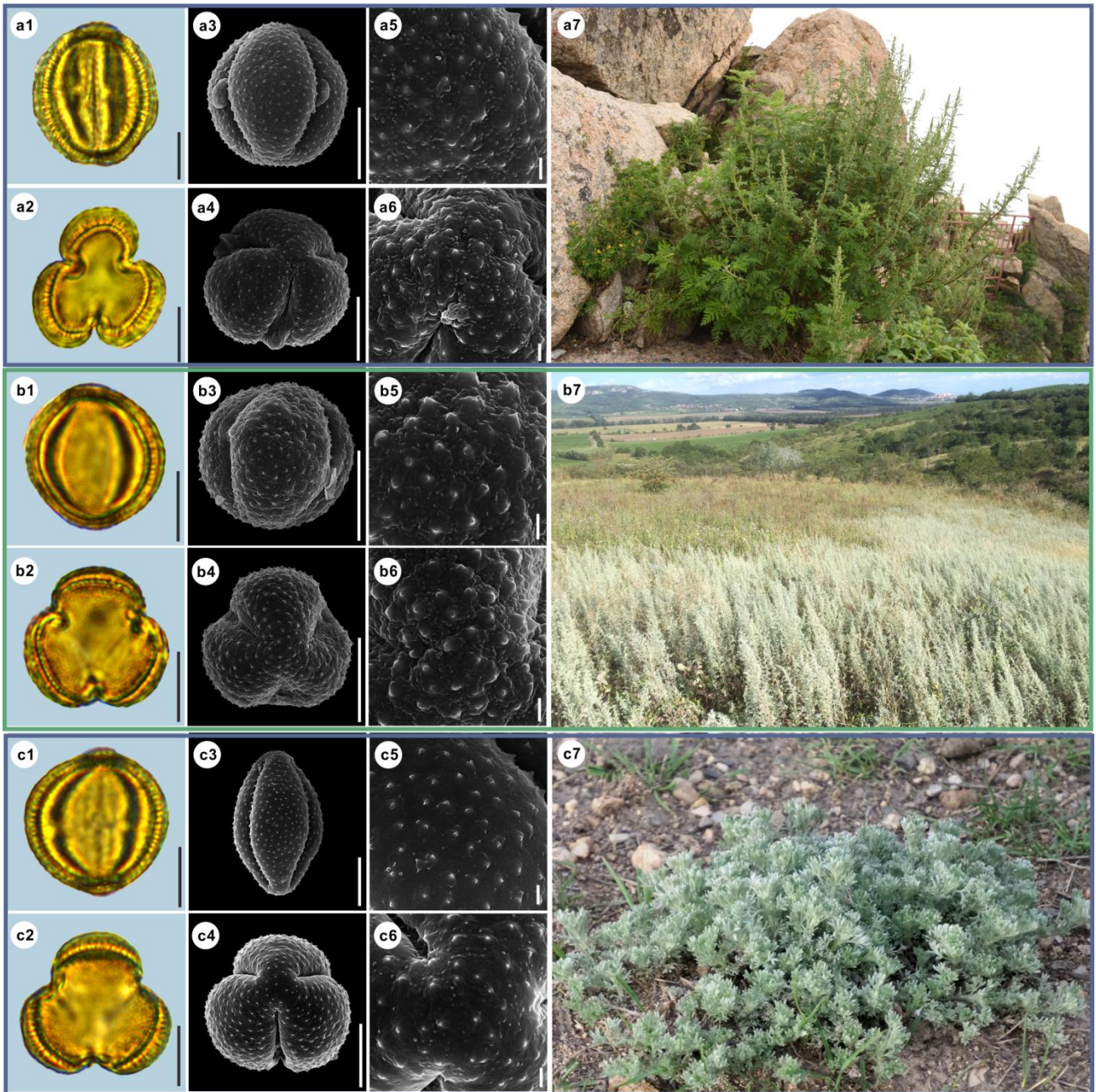
Figure 9. Pollen grains and the habitats of their source plants.

a. *Artemisia stechmanniana*; b. *Artemisia pontica*; c. *Artemisia frigida*.

Pollen grains in equatorial view under LM (a1, b1, c1) and SEM (a3, a5, b3, b5, c3, c5), in polar view under LM (a2, b2, c2) and SEM (a4, a6, b4, b6, c4, c6), along with the habitats of their source plants (a7 provided by © Bo-Han Jiao, b7 cited from https://www.inaturalist.org/photos/93438780 by © Martin Pražák, c7 cited from https://www.inaturalist.org/photos/125022240 by © Suzanne Dingwell).

Scale bar in LM and SEM overview 10 μm, in SEM close-up 1 μm.

229
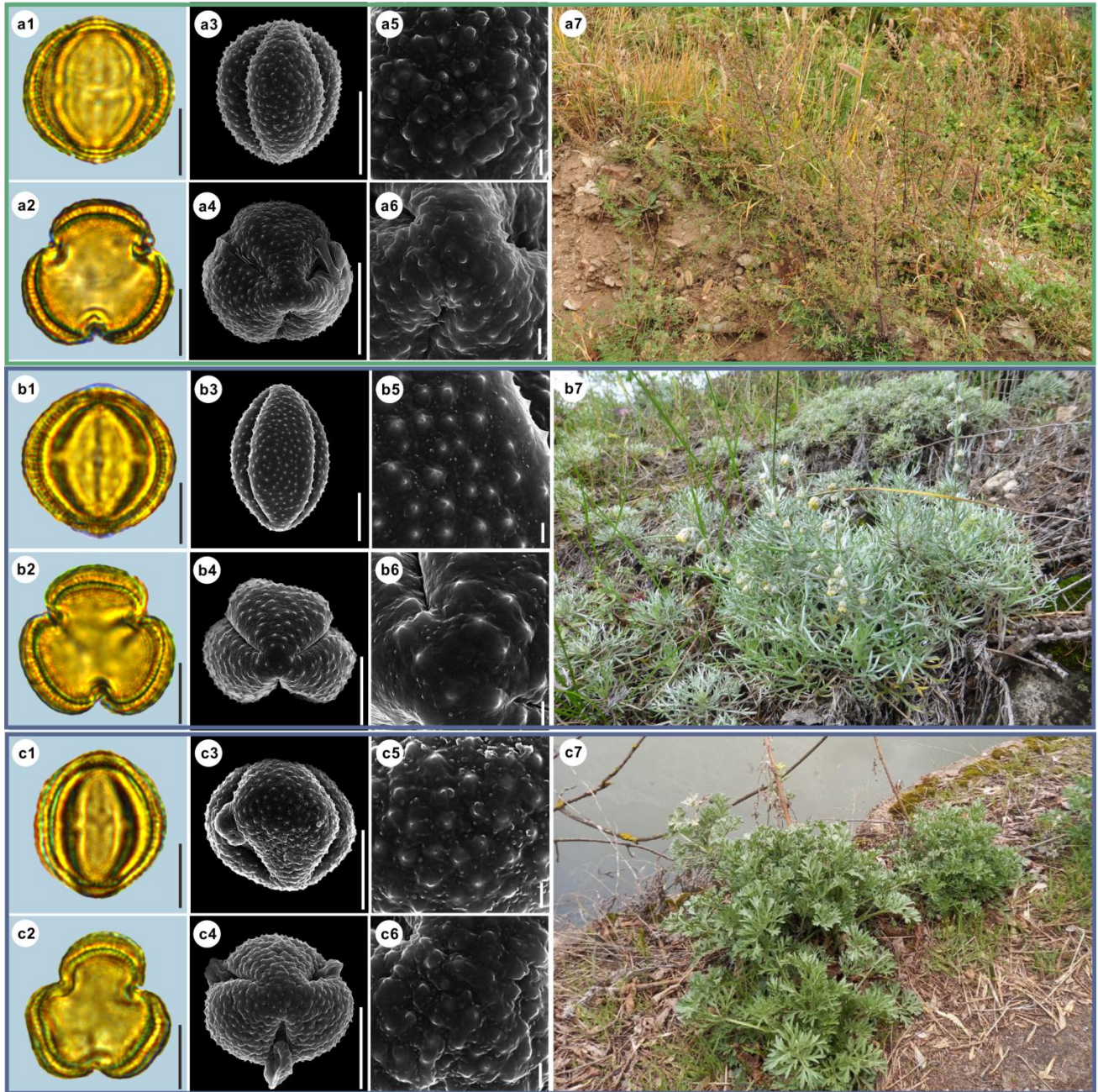
Figure 10. Pollen grains and the habitats of their source plants.

a. *Artemisia rupestris*; b. *Artemisia sericea*; c. *Artemisia absinthium*.

Pollen grains in equatorial view under LM (a1, b1, c1) and SEM (a3, a5, b3, b5, c3, c5), in polar view under LM (a2, b2, c2) and SEM (a4, a6, b4, b6, c4, c6), along with the habitats of their source plants (a7 provided by © Bo-Han Jiao, b7 cited from https://www.inaturalist.org/photos/48033353 by © svetlana_katana, c7 cited from https://www.inaturalist.org/photos/123569286 by © Станислав Лебедев).

Scale bar in LM and SEM overview 10 μm, in SEM close-up 1 μm.
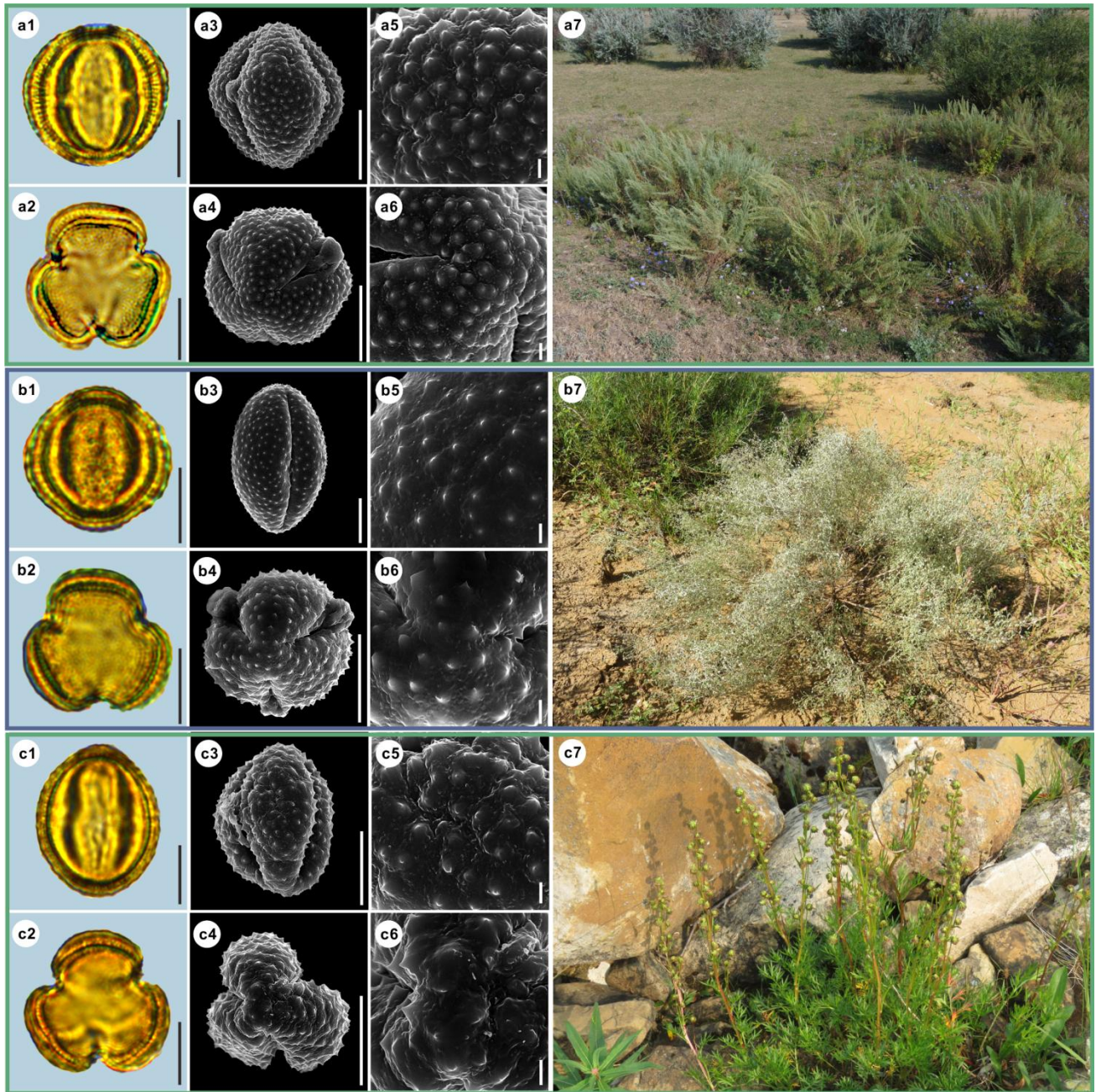
Figure 11. Pollen grains and the habitats of their source plants.

a. *Artemisia abrotanum*; b. *Artemisia blepharolepis*; c. *Artemisia norvegica*.

Pollen grains in equatorial view under LM (a1, b1, c1) and SEM (a3, a5, b3, b5, c3, c5), in polar view under LM (a2, b2, c2) and SEM (a4, a6, b4, b6, c4, c6), along with the habitats of their source plants (a7 cited from https://www.inaturalist.org/photos/116106722 by © Андрей Москвичев, b7 provided by © Ji-Ye Zheng, c7 cited from https://www.inaturalist.org/photos/161393521 by © Erin Springinotic).

Scale bar in LM and SEM overview 10 μm, in SEM close-up 1 μm.
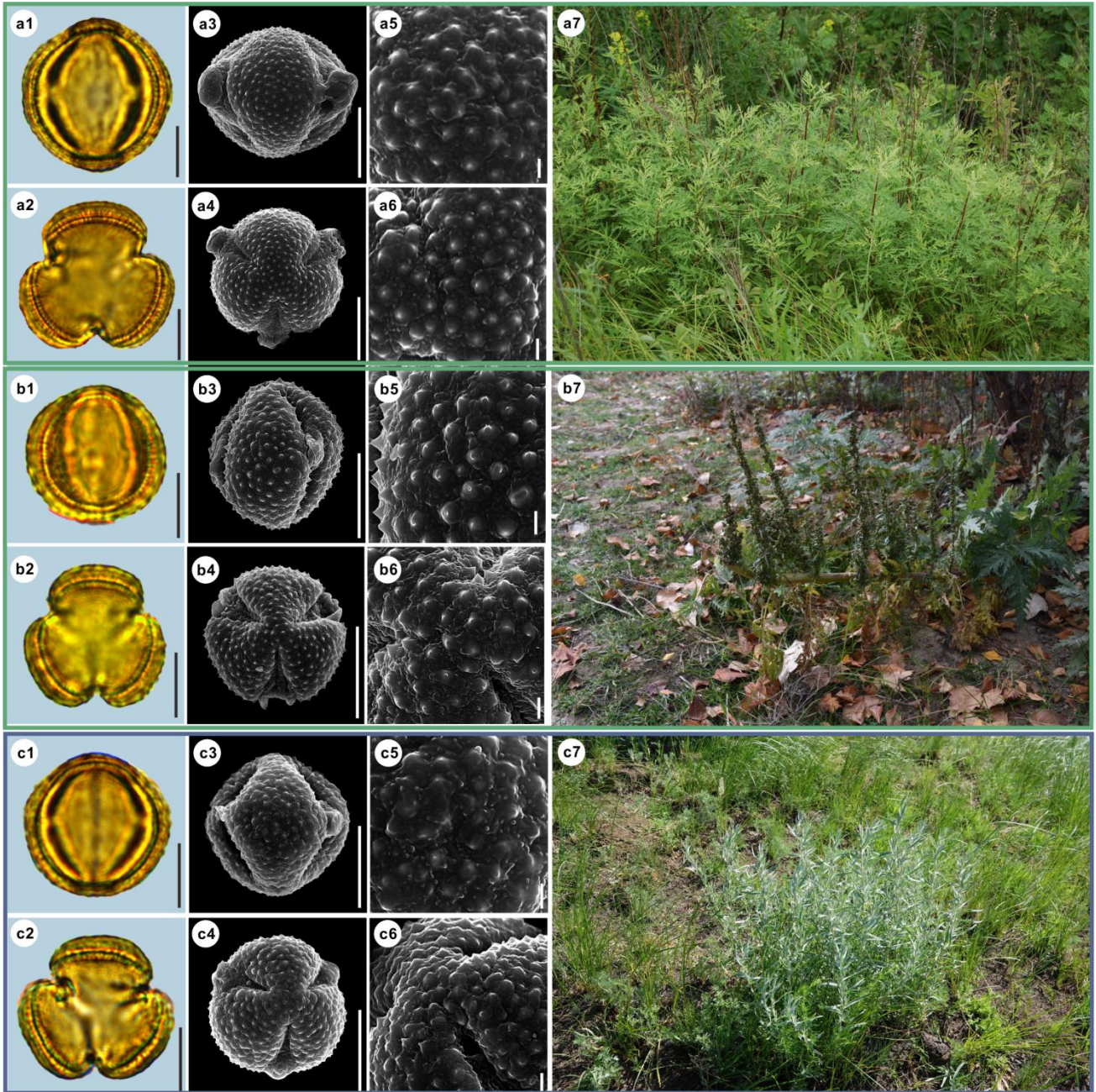
Figure 12. Pollen grains and the habitats of their source plants.

a. *Artemisia tanacetifolia*; b. *Artemisia tournefortiana*; c. *Artemisia dracunculus*.

Pollen grains in equatorial view under LM (a1, b1, c1) and SEM (a3, a5, b3, b5, c3, c5), in polar view under LM (a2, b2, c2) and SEM (a4, a6, b4, b6, c4, c6), along with the habitats of their source plants (a7 cited from https://www.inaturalist.org/photos/78902853 by © Alexander Dubynin, b7 provided by © Chen Chen, c7 cited from https://www.inaturalist.org/photos/76312868 by © anatolymikhaltsov).

Scale bar in LM and SEM overview 10 μm, in SEM close-up 1 μm.

253
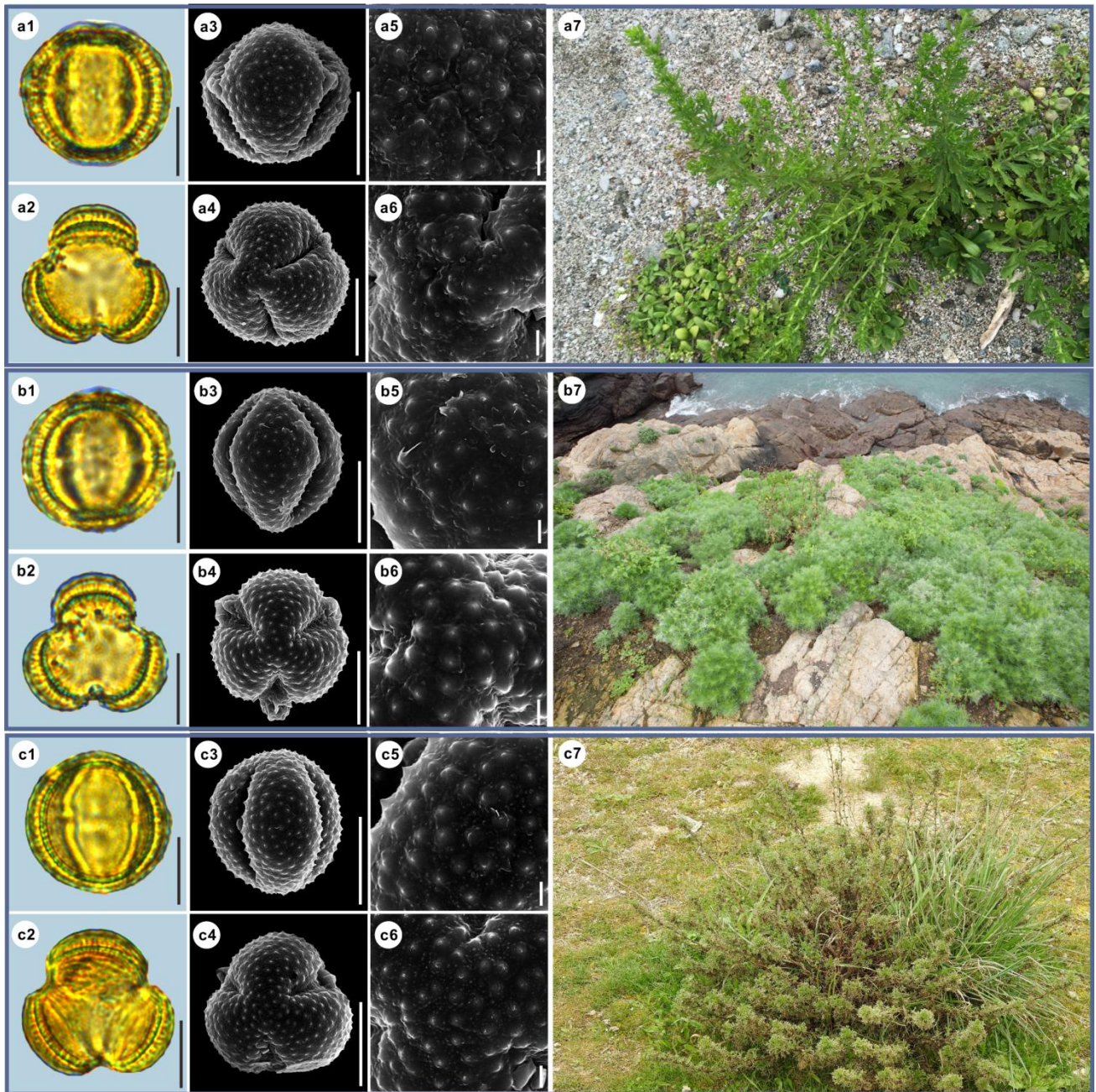
Figure 13. Pollen grains and the habitats of their source plants.

a. *Artemisia japonica*; b. *Artemisia capillaris*; c. *Artemisia campestris*.

Pollen grains in equatorial view under LM (a1, b1, c1) and SEM (a3, a5, b3, b5, c3, c5), in polar view under LM (a2, b2, c2) and SEM (a4, a6, b4, b6, c4, c6), along with the habitats of their source plants (a7 cited from https://www.inaturalist.org/photos/44507659 by © 陳達智 , b7 cited from https://www.inaturalist.org/photos/60639286 by © Cheng-Tao Lin, c7 cited from https://www.inaturalist.org/photos/113822257 by © pedrosanz-anapri).

Scale bar in LM and SEM overview 10 μm, in SEM close-up 1 μm.
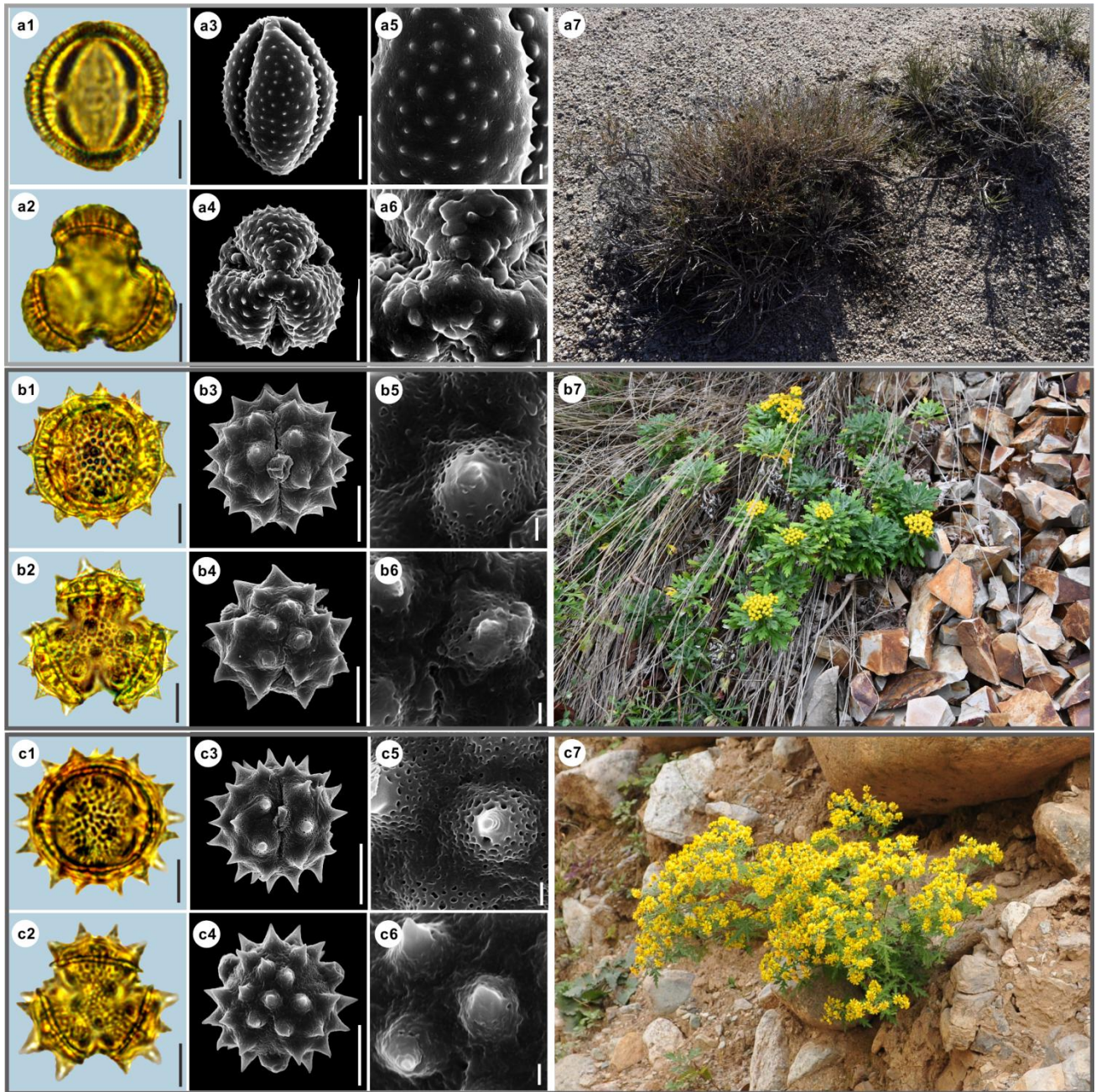
Figure 14. Pollen grains and the habitats of their source plants.

a. *Kaschgaria brachanthemoides*; b. *Ajania pallasiana*; c. *Chrysanthemum indicum*.

Pollen grains in equatorial view under LM (a1, b1, c1) and SEM (a3, a5, b3, b5, c3, c5), in polar view under LM (a2, b2, c2) and SEM (a4, a6, b4, b6, c4, c6), along with the habitats of their source plants (a7 provided by © Chen Chen, b7 cited from https://www.inaturalist.org/photos/162408714 by © Игорь Поспелов, c7 provided by © Bo-Han Jiao).

Scale bar in LM and SEM overview 10 μm, in SEM close-up 1 μm.

3.2 Statistical pollen morphological trait data of 36 sampled taxa

The mean values of 10 pollen morphological traits of 36 sampled species are listed in Table 1, and these data distribution patterns are shown in boxplots (Fig. 15) in the form of variation (25%-75%), and further described in the form of mean value ± standard deviation (M ± SD, Appendix A).

Table 1. Pollen morphological traits of 36 selected species (P: Polar length; E: Equatorial width; T: Exine thickness; L: Pollen length; D: Diameter of spinule base; H: Spinule height; Gs: Granule spacing; Ss: Spinule spacing; Ps: Perforation spacing).

No.	Species	P (μm)	E (μm)	P/E	T (μm)	L (μm)	T/L	D (μm)	H (μm)	D/H	Gs (μm)	Ss (μm)	Gs/Ss	Ps (μm)
1	*Artemisia cana*	23.46	24.5	0.96	3.91	24.58	0.16	0.58	0.46	1.28	0.33	1.60	0.21	0
2	*Artemisia tridentata*	21.36	20.69	1.04	3.55	22.35	0.16	0.76	0.60	1.30	0.24	1.12	0.22	0
3	*Artemisia californica*	18.94	19.13	0.99	2.70	18.85	0.14	0.75	0.71	1.08	0.24	1.45	0.17	0
4	*Artemisia indica*	23.47	23.81	0.99	3.50	23.31	0.15	0.76	0.39	2.04	0.28	1.21	0.24	0
5	*Artemisia argyi*	21.8	21.67	1.01	3.55	22.24	0.16	0.64	0.38	1.71	0.22	0.90	0.26	0
6	*Artemisia mongolica*	21.05	20.42	1.03	3.29	19.78	0.17	0.62	0.41	1.54	0.19	0.91	0.22	0
7	*Artemisia vulgaris*	19.72	19.29	1.03	2.92	18.94	0.16	0.69	0.34	2.13	0.29	1.55	0.20	0
8	*Artemisia selengensis*	20.67	19.68	1.06	3.72	20.8	0.18	0.67	0.38	1.76	0.22	1.05	0.22	0
9	*Artemisia ludoviciana*	21.65	20.82	1.04	3.71	20.94	0.18	0.70	0.37	1.94	0.2	1.23	0.16	0
10	*Artemisia roxburghiana*	23.88	23.69	1.01	3.78	21.81	0.17	0.76	0.39	1.96	0.28	0.79	0.36	0
11	*Artemisia rutifolia*	22.22	22.7	0.98	3.53	24.93	0.14	0.31	0.26	1.2	0.21	1.27	0.17	0
12	*Artemisia chinensis*	21.53	22.75	0.95	2.97	23.71	0.13	0.70	0.55	1.29	0.27	0.91	0.31	0
13	*Artemisia kurramensis*	19.71	19.35	1.02	3.30	19.44	0.17	0.38	0.27	1.41	0.23	1.25	0.19	0
14	*Artemisia compactum*	22.33	21.97	1.02	2.97	21.67	0.14	0.41	0.28	1.50	0.51	0.92	0.56	0
15	*Artemisia maritima*	26.24	23.09	1.14	3.54	24.42	0.14	0.28	0.23	1.30	0.53	1.08	0.50	0
16	*Artemisia aralensis*	22.32	21.91	1.02	3.16	22.76	0.14	0.25	0.22	1.16	0.50	1.09	0.46	0

17	*Artemisia annua*	19.71	19.45	1.02	3.45	19.2	0.18	0.45	0.39	1.18	0.27	1.29	0.21	0
18	*Artemisia freyniana*	23.39	21.3	1.10	3.17	21.29	0.15	0.56	0.40	1.40	0.2	1.15	0.18	0
19	*Artemisia stechmanniana*	26.31	25.16	1.05	3.97	23.45	0.17	0.37	0.35	1.07	0.19	1.40	0.14	0
20	*Artemisia pontica*	20.64	19.62	1.05	3.01	19.75	0.15	0.6	0.37	1.63	0.17	1.32	0.13	0
21	*Artemisia frigida*	25.11	24.9	1.01	4.61	24.83	0.19	0.46	0.32	1.44	0.31	1.3	0.24	0
22	*Artemisia rupestris*	24.45	22.92	1.07	3.18	21.96	0.14	0.55	0.33	1.68	0.25	0.91	0.28	0
23	*Artemisia sericea*	26.31	27.9	0.94	3.75	26.89	0.14	0.89	0.54	1.71	0.28	1.74	0.16	0
24	*Artemisia absinthium*	22.79	20.84	1.09	3.39	19.92	0.17	0.59	0.40	1.52	0.18	1.11	0.16	0
25	*Artemisia abrotanum*	24.47	23.73	1.03	3.15	18.82	0.17	0.72	0.51	1.44	0.22	1.41	0.16	0
26	*Artemisia blepharolepis*	18.96	19.26	0.99	3.15	18.82	0.17	0.69	0.44	1.64	0.37	1.68	0.23	0
27	*Artemisia norvegica*	24.51	22.11	1.11	3.48	22.61	0.15	0.67	0.43	1.66	0.19	1.56	0.12	0
28	*Artemisia tanacetifolia*	28.38	27.75	1.03	3.46	27.63	0.13	0.71	0.32	2.23	0.30	1.08	0.29	0
29	*Artemisia tournefortiana*	20.76	20.43	1.02	3.33	20.03	0.17	0.73	0.42	1.81	0.26	1.25	0.22	0
30	*Artemisia dracunculus*	22.89	22.87	1.00	2.82	21.91	0.13	0.68	0.45	1.56	0.31	0.92	0.34	0
31	*Artemisia japonica*	20.18	21.23	0.95	4.24	21.02	0.2	0.57	0.32	1.8	0.26	1.26	0.21	0
32	*Artemisia capillaris*	19.53	19.64	1.00	3.54	19.18	0.18	0.51	0.36	1.44	0.26	1.27	0.21	0
33	*Artemisia campestris*	21.69	21.26	1.02	3.68	21.21	0.17	0.57	0.38	1.53	0.41	1.23	0.34	0
34	*Kaschagaria brachanthemoides*	23.26	22.09	1.06	3.93	21.01	0.19	0.55	0.44	1.25	0	1.75	0	0.47
35	*Ajania pallasiana*	35.16	35.92	0.98	10.23	38.31	0.27	4.41	3.47	1.29	0	7.84	0	0.39
36	*Chrysanthemum indicum*	33.54	34.42	0.98	8.65	34.82	0.25	2.94	3.59	0.82	0	7.11	0	0.37

277
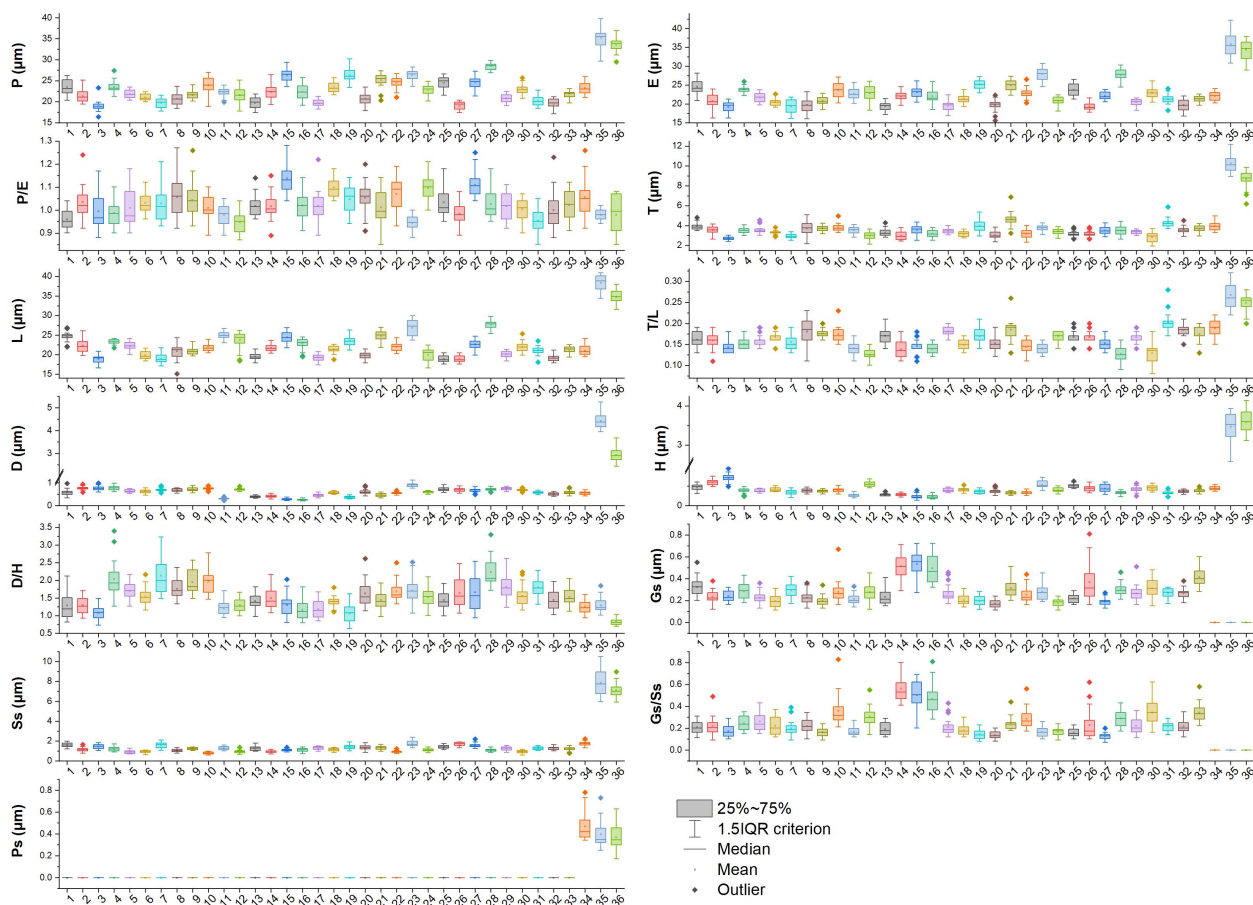
Figure 15. Boxplots of 36 sampled taxa, showing the variations in pollen morphological traits.
1. *Artemisia cana*; 2. *Artemisia tridentata*; 3. *Artemisia californica*; 4. *Artemisia indica*; 5. *Artemisia argyi*; 6. *Artemisia mongolica*; 7. *Artemisia vulgaris*; 8. *Artemisia selengensis*; 9. *Artemisia ludoviciana*; 10. *Artemisia roxburghiana*; 11. *Artemisia rutifolia*; 12. *Artemisia chinensis*; 13. *Artemisia kurramensis*; 14. *Artemisia compactum*; 15. *Artemisia maritima;* 16. *Artemisia aralensis*; 17. *Artemisia annua*; 18. *Artemisia freyniana*; 19. *Artemisia stechmanniana*; 20. *Artemisia pontica*; 21. *Artemisia frigida*; 22. *Artemisia rupestris*; 23. *Artemisia sericea*; 24. *Artemisia absinthium*; 25. *Artemisia abrotanum*; 26. *Artemisia blepharolepis*; 27. *Artemisia norvegica*; 28. *Artemisia tanacetifolia*; 29. *Artemisia tournefortiana*; 30. *Artemisia dracunculus*; 31. *Artemisia japonica*; 32. *Artemisia capillaris*; 33. *Artemisia campestris*; 34. *Kaschagaria brachanthemoides*; 35. *Ajania pallasiana*; 36. *Chrysanthemum indicum*.

3.3 The source plant occurrences

The source plant distributions in global terrestrial biomes of 36 sampled species are shown in Fig. 16. In *Artemisia*, some species have worldwide distributions, such as *A. vulgaris* (Fig. 16-7), *A. absinthium* (Fig. 16-24), and *A. campestris* (Fig. 16-33); a few taxa are limited to East Asia, such as *A. roxburghiana* (Fig. 16-10) and *A. blepharolepis* (Fig. 16-26), while others have narrow and isolated distributions in deserts and xeric shrublands of Central Asia, e.g. *A. kurramensis* (Fig. 16-13) and *A. aralensis* (Fig. 16-16). In outgroups of *Artemisia*, *Kaschagaria brachanthemoides* is also confined to deserts and xeric shrublands of Central Asia (Fig. 16-34), while *Ajania pallasiana* lives in forests of East Asia (Fig. 16-35).

Tropical and Subtropical Moist Broadleaf Forests Tropical and Subtropical Dry Broadleaf Forests Tropical and Subtropical Coniferous Forests
Temperate Broadleaf and Mixed Forests Temperate Coniferous Forests Boreal Forests/Taiga Flooded Grasslands and Savannas
Montane Grasslands and Shrublands Tundra Mediterranean Forests, Woodlands, and Shrub
Tropical and Subtropical Grasslands, Savannas, and Shrublands Temperate Grasslands, Savannas, and Shrublands
Deserts and Xeric Shrublands Mangroves Lakes Rock and Ice

Figure 16. The global distribution maps of 36 sampled taxa in terrestrial biomes (modified from Olson et al., 2001).

1. *Artemisia cana*; 2. *Artemisia tridentata*; 3. *Artemisia californica*; 4. *Artemisia indica*; 5. *Artemisia argyi*; 6. *Artemisia mongolica*; 7. *Artemisia vulgaris*; 8. *Artemisia selengensis*; 9. *Artemisia ludoviciana*; 10. *Artemisia roxburghiana*; 11. *Artemisia rutifolia*; 12. *Artemisia chinensis*; 13. *Artemisia kurramensis*; 14. *Artemisia compactum*; 15. *Artemisia maritima;* 16. *Artemisia aralensis*; 17. *Artemisia annua*; 18. *Artemisia freyniana*; 19. *Artemisia stechmanniana*; 20. *Artemisia pontica*; 21. *Artemisia frigida*; 22. *Artemisia rupestris*; 23. *Artemisia sericea*; 24. *Artemisia absinthium*; 25. *Artemisia abrotanum*; 26. *Artemisia blepharolepis*; 27. *Artemisia norvegica*; 28. *Artemisia tanacetifolia*; 29. *Artemisia tournefortiana*; 30. *Artemisia dracunculus*; 31. *Artemisia japonica*; 32. *Artemisia capillaris*; 33. *Artemisia campestris*; 34. *Kaschagaria brachanthemoides*; 35. *Ajania pallasiana*; 36. *Chrysanthemum indicum*.

4 Potential use of the *Artemisia* pollen datasets

4.1 The pollen classification of *Artemisia*

The pollen grains of Anthemideae and Asteraceae under LM could be simply divided into *Artemisia* pollen type (Figs. 3-13, 14a, Appendix A) with indistinct and short spinules and *Anthemis* pollen type such as *Chrysanthemum indicum* and *Ajania pallasiana* (Figs. 14b-c, Appendix A) with distinct and long spines on pollen exine ornamentation (Wodehouse, 1926; Stix, 1960; Chen, 1987; Chen and Zhang, 1991; Martín et al., 2001; Martín et al., 2003; Sanz et al., 2008; Blackmore et al., 2009; Vallès et al., 2011). *Artemisia* pollen grains are difficult to separate from those of other related genera with *Artemisia* pollen type such as *Kaschgaria brachanthemoides* (Figs. 14a1-2, Appendix A), *Elachanthemum*, *Ajaniopsis*, *Filifolium*, and *Neopallasia* (Chen and Zhang, 1991) under LM due to their great similarity in pollen exine ornamentation and colporate patterns (Chen, 1987; Martín et al., 2001; Martín et al., 2003; Vallès et al., 2011). Furthermore, Sing and Joshi (1969) questioned the feasibility of recognizing pollen types under LM in the highly uniform pollen of *Artemisia*. Later, SEM made it possible to subdivide the pollen of *Artemisia* and those of other related genera within the *Artemisia* pollen type using pollen exine ultrastructure characters (Chen, 1987; Chen and Zhang, 1991; Sun and Xu, 1997; Jiang et al., 2005; Ghahraman et al., 2007; Shan et al., 2007; Hayat et al., 2009; Hayat et al., 2010; Hussain et al., 2019).

Hierarchical cluster analysis (Fig. 17a) revealed that the pollen morphological traits (P/E, H, D, D/H, Ss, Gs, Gs/Ss, and Ps) of *Artemisia* and its outgroups were divided into Clade A with perforations and without granules (Figs. 13a5-6, b5-6, c5-6) and Clade B with granules and without perforations (Figs. 3-13a5-6, b5-6, c5-6) on the pollen exine under SEM.
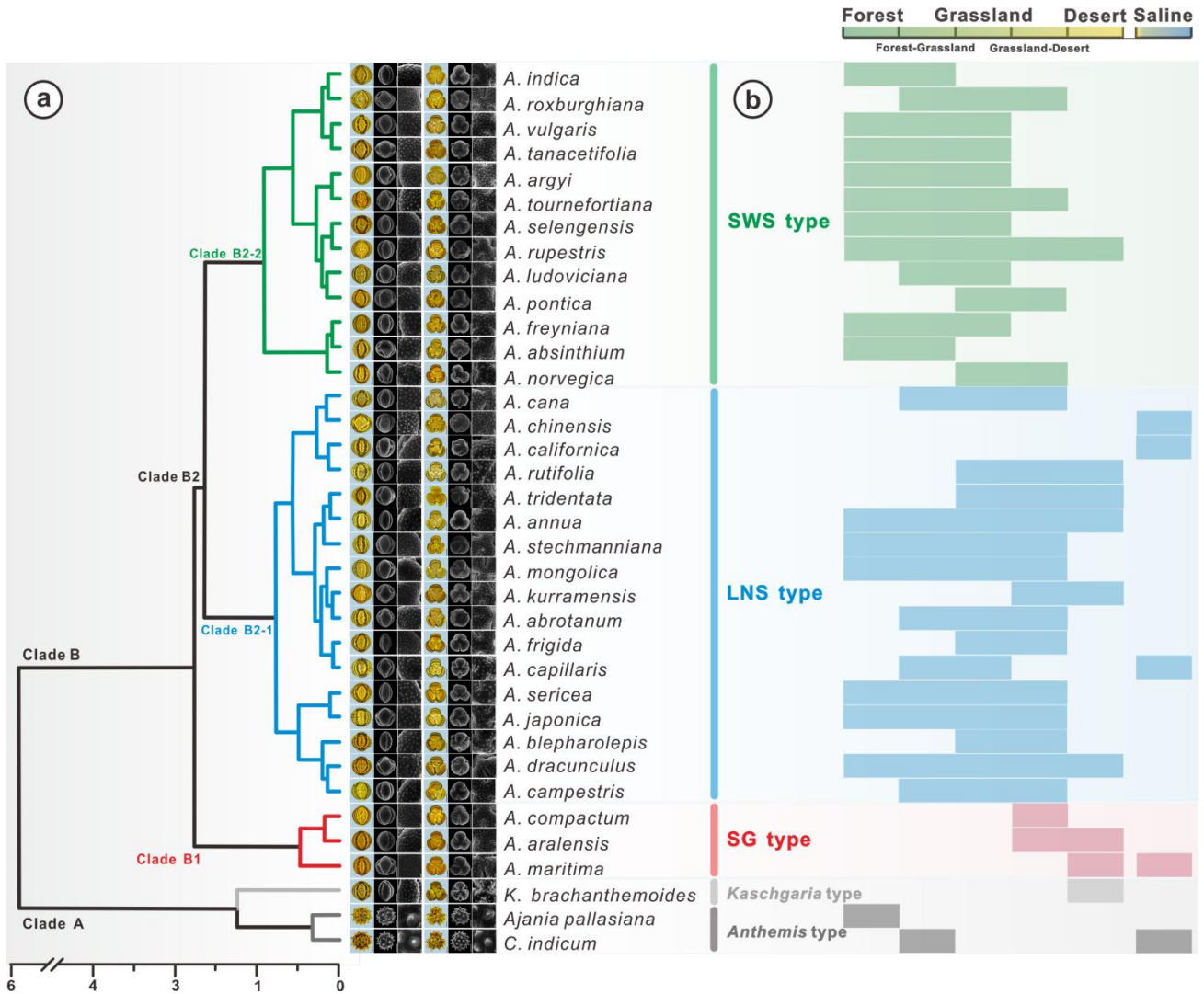
Figure 17. Hierarchical cluster analysis, showing the dendrogram for pollen types from *Artemisia* and outgroups (a) and the habitat ranges of 36 representative species (b, Tutin et al., 1976; Zhang, 2007; Ling et al., 2011).

In addition, Clade A, as the outgroup of *Artemisia*, includes *Anthemis* type (*Chrysanthemum indicum* and *Ajania pallasiana*) with prominent spines on pollen exine under LM, and *Kaschgaria* type (*Kaschgaria brachanthemoides*) with spinules on pollen exine (Figs. 14a, 17a). Clade B comprises three pollen types from three branches of *Artemisia* (Fig. 17a), i.e., SG type (short and wide spinule pollen type, Clade B1), LNS type (long and narrow spinule pollen type, Clade B2-1), and SG type (sparse granule pollen type, Clade B2-2).

Eight pollen morphological traits (P/E, H, D, D/H, Ss, Gs, Gs/Ss, and Ps) were selected for the principal component analysis (PCA) of 36 taxa of *Artemisia* and its outgroups (Fig. 18) and grouped according to the five clades of the cluster analysis, i.e. the five pollen types (Fig. 17a). The results reveal that *Artemisia* pollen morphology differs significantly from that of the outgroups, and that three *Artemisia* pollen types could be distinguished.
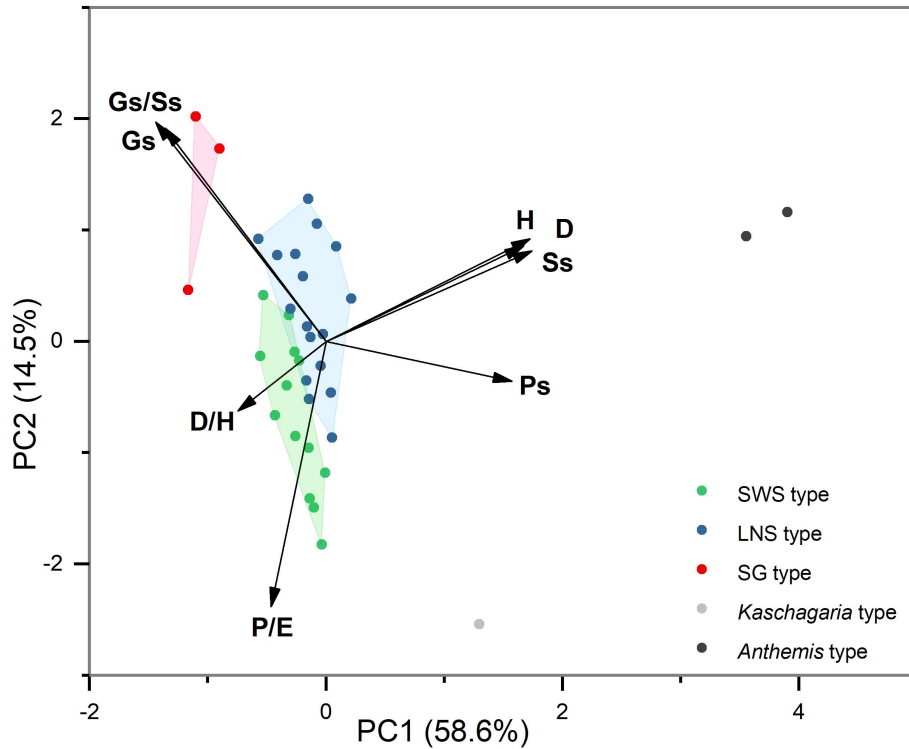
Figure 18. Principal component analysis of 36 taxa of *Artemisia* and its outgroups.

Nine characteristics of *Artemisia* pollen could partially explain the differences between these 3 pollen types (Fig. 19). P/E (the length of polar axis/the length of equatorial axis) in LNS types (0.93-1.06) are significantly different (ANOVA P < 0.001) from both SWS (0.97-1.12) and SG (0.98-1.14), so could be used to identify the LNS type. D/H (diameter of spinule base/spinule height) in the SWS type differ significantly (ANOVA P < 0.001) from both LNS and SG types. The variation range of D/H is 1.38-2.23 in the SWS type, 1.07-1.75 in the LNS type, and 0.98-1.66 in the SG type, indicating that the SWS pollen type is distinguished by short and wide spinules. Gs/Ss (granule spacing/spinule spacing) in the SG type was higher than those of the SWS and LNS types (ANOVA P < 0.001), which distinguished the SG type from the other two types. Moreover, the SG type is characterized by sparse granules with the variation range of Gs/Ss spanning 0.37-0.64, while the SWS and LNS types show much denser granules whose Gs/Ss are mainly below 0.35.

Within the new *Artemisia* pollen classification (Fig. 17a, Key), the SWS type represents a type of pollen with short and wide spinules (D/H > 1.81) and dense granules (Figs. 17a, 19). The LNS type represents a type of pollen with long and narrow spinules (D/H < 1.38) and dense granules (Figs. 17a, 19). The SG type is characterized by sparse granules (Gs/Ss > 0.37) and small, long, and narrow spinules (Figs. 17a, 19).
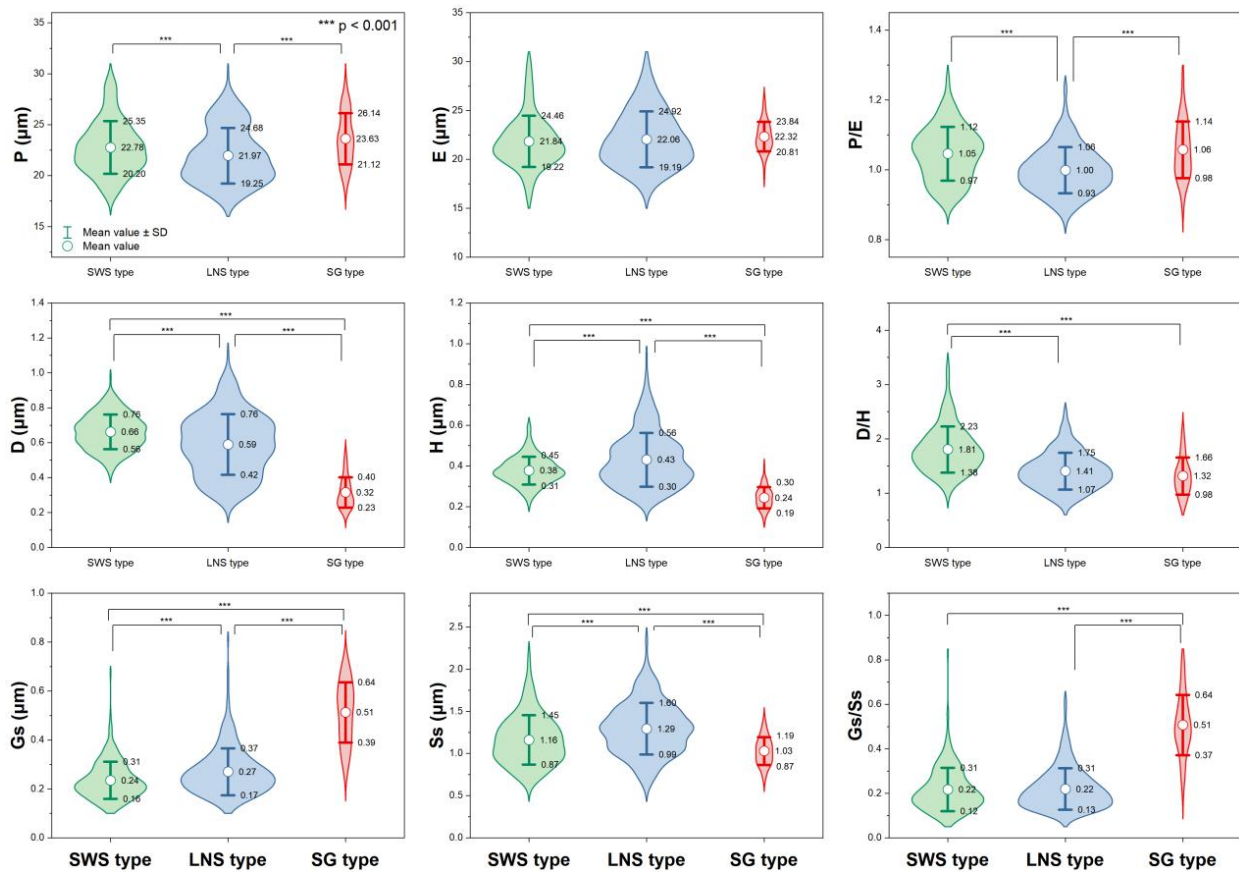
Figure 19. Violin diagrams of three pollen types from *Artemisia*, showing the variations (M ± SD) in nine pollen characters (P: length of polar axis; E: length of equatorial axis; D: diameter of spinule base; H: spinule height; Gs: granule spacing; Ss: spinule spacing; Ps: perforation spacing). Asterisks indicate statistically significant differences (p < 0.001).

4.2 Testing the pollen intraspecific variability within *Artemisia*

Evidence shows that the pollen morphology in *Artemisia* is highly uniform under LM without discrimination (Wodehouse, 1926; Sing and Joshi, 1969; Ling, 1982; Chen, 1987; Wang et al., 1995), which might suggest that statistical analyses of the intraspecific morphological variation of pollen under the LM are limited or meaningless. Right now, the SEM technique has made it possible to subdivide *Artemisia* pollen into different types using pollen exine ultrastructure characters (Chen, 1987; Chen and Zhang, 1991; Sun and Xu, 1997; Jiang et al., 2005; Ghahraman et al., 2007; Shan et al., 2007; Hayat et al., 2009; Hayat et al., 2010; Hussain et al., 2019).

In order to test the intraspecific variability of pollen exine ultrastructure traits, we selected one species respectively from the three pollen types corresponding to the three morphological clades of *Artemisia* pollen, i.e. *Artemisia vulgaris* (SWS type), *Artemisia annua* (LNS type), and *Artemisia maritima* (SG type), and

374 sampled five specimens of each species (Table B2). Six pollen traits, i.e. D, H, D/H, Gs, Ss, and Gs/Ss, were

375 counted and analysed under SEM to test for intraspecific variability of pollen exine ultrastructure traits.

376   The test showed that it was feasible to use stable D/H and Gs/Ss for pollen type classification of

377 *Artemisia* because 1) D/H and Gs/Ss were stable within species (Figure R220, Table R2) for the pollen

378 classification; 2) D, H, Gs, and Ss were variable as size values, e.g. these four traits were significantly

379 different within species in both *A. vulgaris* and *A. annua*, while D, H, and Ss were significantly different

380 within species in *A. maritima* (Figure R220, Table R2). There was evidence showing that size values such as

381 pollen exine ultrastructure size were often variable within species due to their genetic divergence, various

382 habitats, and different experimental treatments (Mo et al., 1997; Zhao and Yao, 1999; Zhang and Qian, 2011).
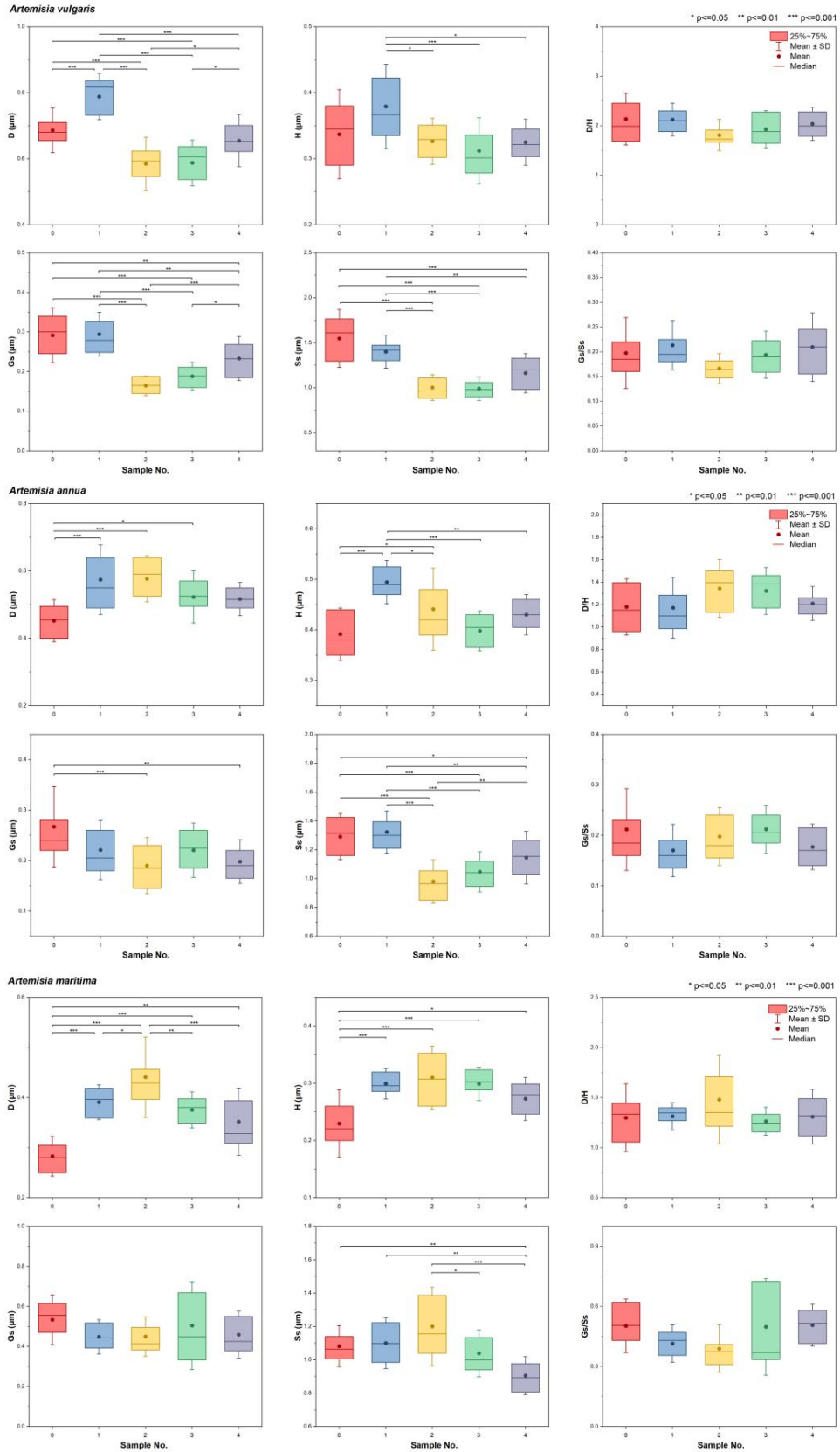
Figure 20. Boxplots of intraspecific pollen exine ultrastructure characters from three species of *Artemisia*, showing the variations (M ± SD) in six pollen characters (D: diameter of spinule base; H: spinule height; Gs: granule spacing; Ss: spinule spacing; Ps: perforation spacing). Asterisks indicate statistically significant differences (*p <= 0.05, **p <= 0.01, ***p < 0.001).

Table 2. The results of ANOVA for intraspecific variability in pollen exine ultrastructure characters among three representative species.

Pollen exine ultrastructure characters	SWS type	LNS type	SG type
	Artemisia vulgaris	*Artemisia annua*	*Artemisia maritima*
D (μm)	significant	significant	significant
H (μm)	significant	significant	significant
D/H	non-significant	non-significant	non-significant
Gs (μm)	significant	significant	significant
Ss (μm)	significant	significant	significant
Gs/Ss	non-significant	non-significant	non-significant

Key to 3 pollen types of *Artemisia* and 3 outgroups

1. Pollen exine with perforations and without granules under SEM …………………………………………2

1. Pollen exine with granules and without perforations under SEM …………………………………………3

2. Distinct and long spines on pollen exine, with H > 3 μm………………………………………………*Anthemis* type

2. Indistinct and short spinules on pollen exine, with H < 1μm…………………………………*Kaschgaria* type

3. Pollen exine with sparse granules and Gs/Ss ≥ 0.37 under SEM ………………………………………SG type

3. Pollen exine with dense granules and Gs/Ss ≤ 0.31 under SEM…………………………………………4

4. Pollen exine with D/H < 1.38 under SEM……………………………………………………………LNS type

4. Pollen exine with D/H ≥ 1.38 under SEM……………………………………………………………SWS type

4.~~2~~3 The ecological implications of *Artemisia* pollen types

Plotting the distribution data of 33 species from 9 main branches of *Artemisia* constrained by the phylogenetic framework (Fig. 1) onto the global terrestrial biomes (Fig. 2~~0~~1), we noticed that the genus is widely

411 distributed from forest to grassland, desert, and saline habitats (Figs. 16, 17b, 2~~0~~1). Furthermore, different

412 species of *Artemisia* with SWS pollen type (Fig. 2~~0~~1a) and LNS type (Fig. 2~~0~~1b) have a rather wide

413 distribution with severely overlapping ranges while those with SG type (Fig. 2~~0~~1c) have narrow and isolated

414 distributions.

415
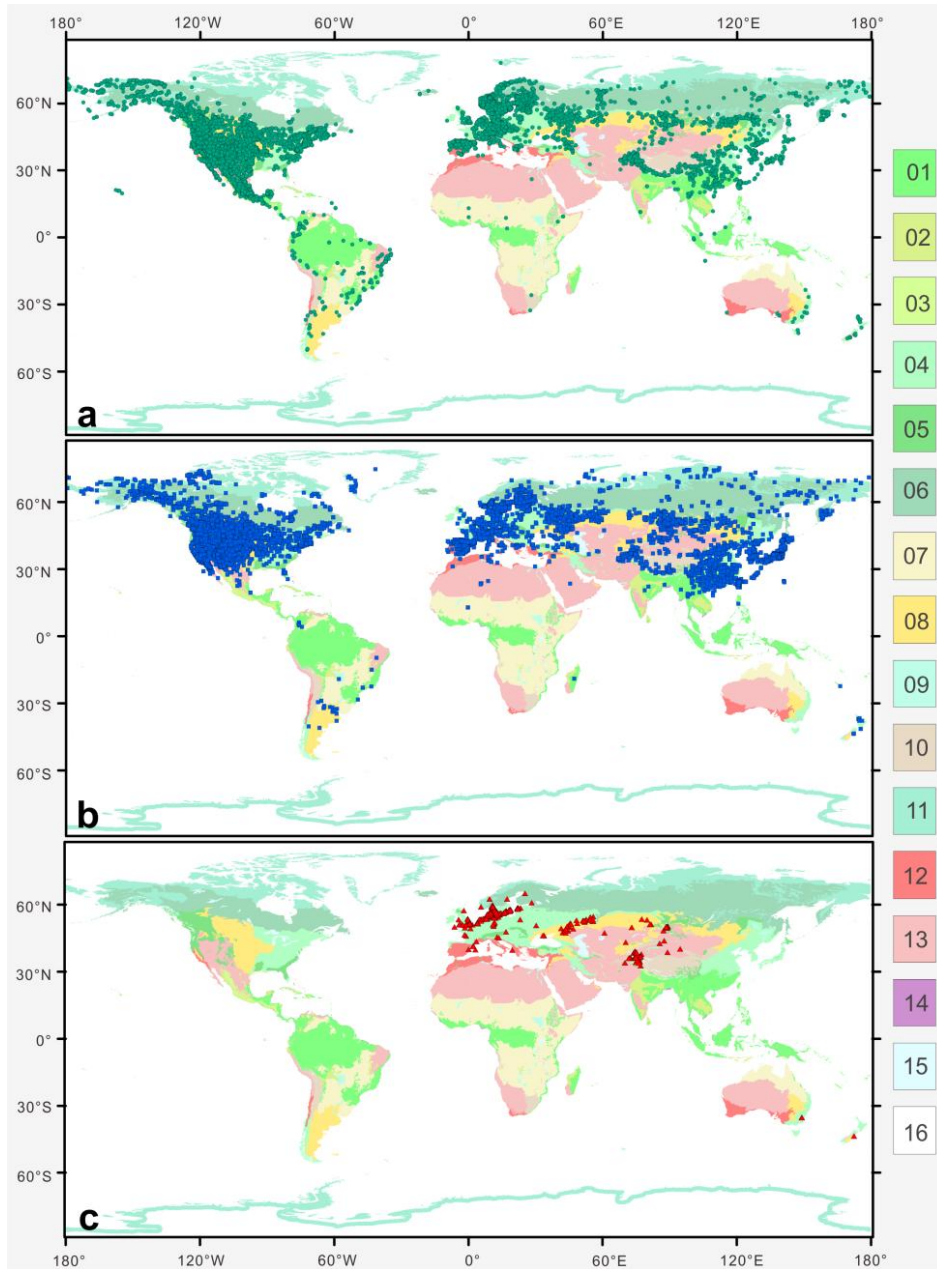
Figure 2~~10~~. The global distribution pattern of 3 *Artemisia* pollen types in terrestrial biomes (modified from Olson et al., 2001). a. SG type; b. LNS type; c. SWS type.

14 terrestrial biomes: 01. Tropical and Subtropical Moist Broadleaf Forests; 02. Tropical and Subtropical Dry Broadleaf Forests; 03. Tropical and Subtropical Coniferous Forests; 04. Temperate Broadleaf and Mixed Forests; 05. Temperate Coniferous Forests; 06. Boreal Forests/Taiga; 07. Flooded Grasslands and Savannas; 08. Montane Grasslands and Shrublands; 09. Tundra; 10: Mediterranean Forests, Woodlands, and Shrub; 11.

422 Tropical and Subtropical Grasslands, Savannas, and Shrublands; 12. Temperate Grasslands, Savannas, and
423 Shrublands; 13. Deserts and Xeric Shrublands; 14. Mangroves; 15. Lakes; 16. Rock and Ice.

424   The ecological implications of *Artemisia* pollen types mentioned above fall into four categories. (i)

425 *Artemisia* with the SG pollen type all belong to the subg. *Seriphidium*, which generally grows in dry habitats

426 ranging from grassland desert to desert and coastal saline-alkaline environments, with their distribution

427 largely limited to Eurasia and growing at low altitude (Figs. 17b, 2~~0~~1c, 2~~1~~2). (ii) The habitats of *Artemisia*

428 with LNS pollen type have a global distribution and occur in forest, grassland and desert, and even coastal

429 areas (Figs. 17b, 2~~0~~1b, 2~~1~~2), with the highest mean annual temperature (MAT). Hence, the LNS pollen type is

430 a generalist. (iii) *Artemisia* with SWS pollen type include Sect. *Artemisia* and its habitats range from forest to

431 desert, although most of the taxa are confined to humid environments from forest to grassland with a global

432 distribution and the highest mean annual precipitation (MAP, Figs. 17b, 2~~0~~1c, 2~~1~~2). (iv) If the SWS pollen

433 type and the SG pollen type appear together, the range of vegetation types could be reduced to grassland

434 desert and desert through niche coexistence (Fig. 17b).
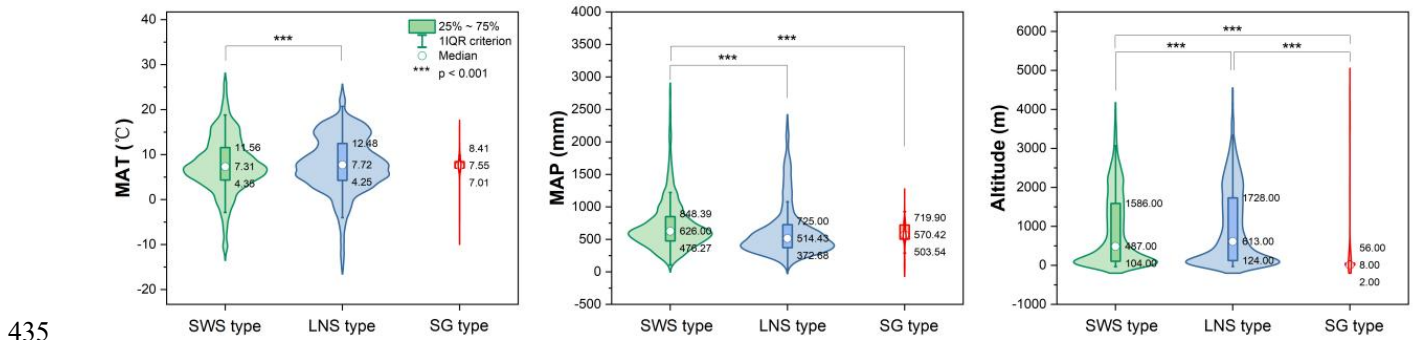
435

436 **Figure 2~~1~~2.** Violin diagrams of three pollen types from *Artemisia*, showing the variations (25%-75%) in MAT,
437 MAP, and altitude. Asterisks indicate statistically significant differences (p < 0.001).

438   In addition, we noticed that *Kaschgaria brachanthemoides* as an outgroup of *Artemisia* lives in dry

439 mountain valleys or dry riverbeds of Northwest China (Toksun) and Kazakhstan, with highly characteristic

440 pollen (Fig. 14a), narrow habitats (Fig. 17b), and regional distribution (Fig. 16-34) and has the potential to

441 indicate some specific habitats.

442 **5 Data availability**

443 Pollen datasets (Table 3~~2~~) including pollen photographs under LM and SEM, statistical data of pollen

444 morphological traits, and their source plant distribution for each species are available at Zenodo

445 (https://doi.org/10.5281/zenodo.6900308~~6791891~~; Lu et al., 2022).

446 **Table 3~~2~~.** *Artemisia* pollen datasets in this study.

Data type	Data format	Data acquisition	Data accessibility
The phylogenetic framework of *Artemisia* pollen sampling.	.png	Literature survey (modified from Malik et al., 2017).	This article
A voucher specimen list of 36 representative species.	.doc	Pollen samples were obtained from PE herbarium at the Institute of Botany, Chinese Academy of Sciences.	
12 illustrations of pollen grains and the habitats of their source plants.	.png	Habitat photos from online sources (Appendix Table A).	
4018 original pollen photographs (3205 under LM, 813 under SEM).	.jpg	Pollen samples were acetolyzed by the standard method and fixed in glycerine jelly. The pollen grains were photographed under LM and SEM using standard procedures.	
9360 pollen morphological trait measurements~~statistical pollen morphological traits.~~ of 36 representative species.	.xlsx	Statistical data of pollen morphological traits were measured by standard methods.	Zenodo (https://doi.org/10.5281/zenodo.6900308~~67 91891~~; Lu et al., 2022)
1800 pollen morphological trait measurements for testing the pollen intraspecific variability within *Artemisia*.	.xlsx	Statistical data of pollen morphological traits were measured by standard methods.	
30858 source plant occurrence information, and corresponding environmental factors including altitude and 19 climate parameters.	.xlsx	Their source plant distribution coordinates were obtained from GBIF (https://doi.org/10.15468/dl.596xd9). The corresponding environmental factors of these coordinates were obtained from WorldClim (https://www.worldclim.org/) with a spatial resolution of 30 seconds between 1970-2000.	

447 **6 Summary**

To cover the maximum range of *Artemisia* pollen morphological variation, we provide a pollen dataset of 36 species from 9 clades and 3 outgroups of *Artemisia* constrained by the phylogenetic framework, containing high-quality pollen photographs under LM and SEM, statistical data of pollen morphological traits, together with their source plant distribution, and corresponding environmental factors. Here, we attempt to decipher the underlying causes of the long-standing disagreement in the palynological community on the correlation between *Artemisia* pollen and aridity by recognizing the different ecological implications of *Artemisia* pollen types.

This dataset should work well for identifying and classifying *Artemisia* pollen from Neogene and Quaternary sediments. While *Artemisia* pollen grains are uniform in morphology under LM, different types can be recognized under SEM. So, the single-grain technique for picking out fossil pollen grains and photographing the same grains under LM and SEM should provide valuable insights in the diversity of fossil *Artemisia* (Ferguson et al., 2007; Grímsson et al., 2011; Grímsson et al., 2012; Halbritter et al., 2018). Furthermore, those *Artemisia* pollen grains could then be compared with the rich photographs from this dataset, and together with the key provided here, possibly attributed to one of the three *Artemisia* pollen types, which in turn may provide a link to the different habitat ranges.

However, the application of this dataset probably may not work well for the Palaeogene, as 1) *Artemisia* might have originated in the Palaeocene, although there is no evidence for a specific location or time interval of its origin (e.g. Ling 1982; Wang 2004; Miao 2011); 2) both the lack of macrofossils of *Artemisia* and the strong pollen similarity between *Artemisia* and its closely related taxa under LM might lead to confusion and more uncertainty in tracing the origin of *Artemisia*. On the other hand, the present dataset provides a potential morphological tool to distinguish *Artemisia* pollen grains from those of its related taxa at the SEM level and may shed light on the origin of this genus in the Palaeogene.

Moreover, these pollen photographs also have potential and the possibility to be used for deep learning research. We are attempting to automatically identify pollen images using pollen assemblages from the eastern Central Asian desert as an example with deep convolutional neural network (DCNN) of artificial intelligence. Pollen images of the many species of *Artemisia* provided here, and the increasing number of intraspecific replications in the future, will all serve for projected image identification research.

Finally and most importantly, the *Artemisia* pollen dataset as designed is open and expandable for new pollen data from *Artemisia* worldwide in order to better serve the global environment assessment and refined reconstruction of vegetation in the geological past as a basis or blueprint for other overarching statistical

478   analyses on pollen morphology.

Appendix A

480 **Text A1**

481 Pollen morphological descriptions of 36 representative species from 9 clades of *Artemisia* and 3 outgroups.

482 Pollen morphology of *Artemisia*: pollen grains oblate, spherical, or ellipsoidal; apertures tricolporate; almost
483 circular in equatorial view and trilobate circular in polar view; the exine near the colpi gradually thinned; the
484 exine has an obvious double structure of inner and outer layers where the outer is thicker than the inner under
485 LM; the exine ornamentation is psilate (LM), spinulate and granule (SEM).

486 **1. *Artemisia cana* (Table 1, Figs. 3a, 15)**

487 Pollen grains spheroidal or oblate. Almost circular in equatorial view and trilobate circular in polar view.
488 Apertures tricolporate. The exine near the colpi gradually thinned. Polar length (P) = 23.46 ± 1.76 μm (M ±
489 SD), equatorial width (E) = 24.50 ± 2.13 μm (M ± SD), P/E = 0.96 ± 0.04 (M ± SD), Exine thickness (T) =
490 3.91 ± 0.36 μm (M ± SD), Pollen length (L) = 24.58 ± 1.24 μm (M ± SD), T/L = 0.16 ± 0.02. The exine
491 ornamentation is psilate (LM), spinulate (SEM). Under SEM, diameter of spinule base (D) = 0.58 ± 0.13 μm
492 (M ± SD), spinule height (H) = 0.46 ± 0.08 μm (M ± SD), D/H = 1.28 ± 0.38 (M ± SD), granule spacing (Gs)
493 = 0.33 ± 0.08 μm (M ± SD), spinule spacing (Ss) = 1.60 ± 0.22 μm (M ± SD), Gs/Ss = 0.21 ± 0.06 (M ± SD).

494 Habitat: grasslands, gravel soils, mountain meadows, stream banks; Wet mountain meadows, stream banks,
495 rocky areas with late-lying snows.

496 **2. *Artemisia tridentata* (Table 1, Figs. 3b, 15)**

497 Pollen grains prolate or spheroidal. Almost circular in equatorial view and trilobate circular in polar view.
498 Apertures tricolporate. The exine near the colpi gradually thinned. P = 21.36 ± 1.54 μm, E = 20.69 ± 1.85 μm,
499 P/E = 1.04 ± 0.07, T = 3.55 ± 0.41 μm, L = 22.35 ± 1.90 μm, T/L = 0.16 ± 0.02. The exine ornamentation is
500 psilate (LM), spinulate (SEM). Under SEM, D = 0.76 ± 0.08 μm, H = 0.60 ± 0.08 μm, D/H = 1.30 ± 0.23, Gs
501 = 0.24 ± 0.06 μm, Ss = 1.12 ± 0.22 μm, Gs/Ss = 0.22 ± 0.08.

502 Habitat: mountains, grasslands, and meadows of western North America. Arid and semi-arid, desert, or
503 semi-desert areas of the growing shrub or semi-shrub environment.

504 **3. *Artemisia californica* (Table 1, Figs. 3c, 15)**

505 Pollen grains prolate or spheroidal or oblate. Almost circular in equatorial view and trilobate circular in polar
506 view. Apertures tricolporate. The exine near the colpi gradually thinned. P = 18.94 ± 1.30 μm, E = 19.13 ±
507 1.43 μm, P/E = 0.99 ± 0.08, T = 2.70 ± 0.16 μm, L = 18.85 ± 1.12 μm, T/L = 0.14 ± 0.01. The exine
508 ornamentation is psilate (LM), spinulate (SEM). Under SEM, D = 0.75 ± 0.11 μm, H = 0.71 ± 0.10 μm, D/H =
509 1.08 ± 0.20, Gs = 0.24 ± 0.05 μm, Ss = 1.45 ± 0.23 μm, Gs/Ss = 0.17 ± 0.05.

510   Habitat: coastal scrub, dry foothills.

511   **4. *Artemisia indica* (Table 1, Figs. 4a, 15)**

512   Pollen grains spheroidal or oblate. Almost circular in equatorial view and trilobate circular in polar view.

513   Apertures tricolporate. The exine near the colpi gradually thinned. $P = 23.47 \pm 1.39$ μm, $E = 23.81 \pm 0.86$ μm,

514    $P/E = 0.99 \pm 0.06$, $T = 3.50 \pm 0.27$ μm, $L = 23.31 \pm 0.61$ μm, $T/L = 0.15 \pm 0.01$. The exine ornamentation is

515   psilate (LM), spinulate (SEM). Under SEM, $D = 0.76 \pm 0.10$ μm, $H = 0.39 \pm 0.06$ μm, $D/H = 2.04 \pm 0.53$, Gs

516    $= 0.28 \pm 0.07$ μm, $Ss = 1.21 \pm 0.24$ μm, $Gs/Ss = 0.24 \pm 0.07$.

517   Habitat: roadsides, forest margins, slopes, shrublands; low elevations to 2000 m.

518   **5. *Artemisia argyi* (Table 1, Figs. 4b, 15)**

519   Pollen grains prolate or spheroidal. Almost circular in equatorial view and trilobate circular in polar view.

520   Apertures tricolporate. The exine near the colpi gradually thinned. $P = 21.80 \pm 1.00$ μm, $E = 21.67 \pm 1.27$ μm,

521    $P/E = 1.01 \pm 0.08$, $T = 3.55 \pm 0.40$ μm, $L = 22.24 \pm 1.13$ μm, $T/L = 0.16 \pm 0.01$. The exine ornamentation is

522   psilate (LM), spinulate (SEM). Under SEM, $D = 0.64 \pm 0.07$ μm, $H = 0.38 \pm 0.04$ μm, $D/H = 1.71 \pm 0.23$, Gs

523    $= 0.22 \pm 0.06$ μm, $Ss = 0.90 \pm 0.17$ μm, $Gs/Ss = 0.26 \pm 0.09$.

524   Habitat: waste places, roadsides, slopes, hills, steppes, forest steppes; low elevations to 1500 m.

525   **6. *Artemisia mongolica* (Table 1, Figs. 4c, 15)**

526   Pollen grains prolate or spheroidal. Almost circular in equatorial view and trilobate circular in polar view.

527   Apertures tricolporate. The exine near the colpi gradually thinned. $P = 21.05 \pm 0.82$ μm, $E = 20.42 \pm 1.01$ μm,

528    $P/E = 1.03 \pm 0.05$, $T = 3.29 \pm 0.19$ μm, $L = 19.78 \pm 0.99$ μm, $T/L = 0.17 \pm 0.01$. The exine ornamentation is

529   psilate (LM), spinulate (SEM). Under SEM, $D = 0.62 \pm 0.08$ μm, $H = 0.41 \pm 0.05$ μm, $D/H = 1.54 \pm 0.25$, Gs

530    $= 0.19 \pm 0.06$ μm, $Ss = 0.91 \pm 0.14$ μm, $Gs/Ss = 0.22 \pm 0.08$.

531   Habitat: slopes, shrublands, riverbanks, lakeshores, roadsides, steppes, forest steppes, dry valleys; low

532   elevations to 2000 m.

533   **7. *Artemisia vulgaris* (Table 1, Figs. 5a, 15)**

534   Pollen grains prolate or spheroidal. Almost circular in equatorial view and trilobate circular in polar view.

535   Apertures tricolporate. The exine near the colpi gradually thinned. $P = 19.72 \pm 1.25$ μm, $E = 19.29 \pm 1.82$ μm,

536    $P/E = 1.03 \pm 0.08$, $T = 2.92 \pm 0.23$ μm, $L = 18.94 \pm 1.09$ μm, $T/L = 0.16 \pm 0.02$. The exine ornamentation is

537   psilate (LM), spinulate (SEM). Under SEM, $D = 0.69 \pm 0.07$ μm, $H = 0.34 \pm 0.07$ μm, $D/H = 2.13 \pm 0.52$, Gs

538    $= 0.29 \pm 0.07$ μm, $Ss = 1.55 \pm 0.32$ μm, $Gs/Ss = 0.20 \pm 0.07$.

539   Habitat: roadsides, slopes, canyons, forest margins, forest steppes, subalpine steppes; 1500-3800 m.

540   **8. *Artemisia selengensis* (Table 1, Figs. 5b, 15)**

541 Pollen grains prolate or spheroidal. Almost circular in equatorial view and trilobate circular in polar view.

542 Apertures tricolporate. The exine near the colpi gradually thinned. P = 20.67 ± 1.57 μm, E = 19.68 ± 1.94 μm,

543 P/E = 1.06 ± 0.09, T = 3.72 ± 0.72 μm, L = 20.80 ± 2.21 μm, T/L = 0.18 ± 0.03. The exine ornamentation is

544 psilate (LM), spinulate (SEM). Under SEM, D = 0.67 ± 0.08 μm, H = 0.38 ± 0.05 μm, D/H = 1.76 ± 0.27, Gs

545 = 0.22 ± 0.06 μm, Ss = 1.05 ± 0.15 μm, Gs/Ss = 0.22 ± 0.07.

546 Habitat: riverbanks, lakeshores, humid areas, meadows, slopes, roadsides.

547 **9.** *Artemisia ludoviciana* **(Table 1, Figs. 5c, 15)**

548 Pollen grains prolate or spheroidal. Almost circular in equatorial view and trilobate circular in polar view.

549 Apertures tricolporate. The exine near the colpi gradually thinned. P = 21.65 ± 1.02 μm, E = 20.82 ± 1.10 μm,

550 P/E = 1.04 ± 0.08, T = 3.71 ± 0.28 μm, L = 20.94 ± 1.13 μm, T/L = 0.18 ± 0.01. The exine ornamentation is

551 psilate (LM), spinulate (SEM). Under SEM, D = 0.70 ± 0.08 μm, H = 0.37 ± 0.04 μm, D/H = 1.94 ± 0.31, Gs

552 = 0.20 ± 0.05 μm, Ss = 1.23 ± 0.13 μm, Gs/Ss = 0.16 ± 0.04.

553 Habitat: disturbed roadsides, open meadows, rocky slopes.

554 **10.** *Artemisia roxburghiana* **(Table 1, Figs. 6a, 15)**

555 Pollen grains prolate or spheroidal. Almost circular in equatorial view and trilobate circular in polar view.

556 Apertures tricolporate. The exine near the colpi gradually thinned. P = 23.88 ± 2.04 μm, E = 23.69 ± 2.00 μm,

557 P/E = 1.01 ± 0.06, T = 3.78 ± 0.39 μm, L = 21.81 ± 1.05 μm, T/L = 0.17 ± 0.02. The exine ornamentation is

558 psilate (LM), spinulate (SEM). Under SEM, D = 0.76 ± 0.07 μm, H = 0.39 ± 0.06 μm, D/H = 1.96 ± 0.37, Gs

559 = 0.28 ± 0.11 μm, Ss = 0.79 ± 0.11 μm, Gs/Ss = 0.36 ± 0.14.

560 Habitat: roadsides, slopes, dry canyons, grasslands, waste areas, terraces; 700-3900 m.

561 **11.** *Artemisia rutifolia* **(Table 1, Figs. 6b, 15)**

562 Pollen grains spheroidal or oblate. Almost circular in equatorial view and trilobate circular in polar view.

563 Apertures tricolporate. The exine near the colpi gradually thinned. P = 22.22 ± 1.10 μm, E = 22.70 ± 1.37 μm,

564 P/E = 0.98 ± 0.05, T = 3.53 ± 0.37 μm, L = 24.93 ± 1.05 μm, T/L = 0.14 ± 0.01. The exine ornamentation is

565 psilate (LM), spinulate (SEM). Under SEM, D = 0.31 ± 0.04 μm, H = 0.26 ± 0.04 μm, D/H = 1.20 ± 0.18, Gs

566 = 0.21 ± 0.05 μm, Ss = 1.27 ± 0.19 μm, Gs/Ss = 0.17 ± 0.04.

567 Habitat: hills, dry river valleys, basins, steppes, semideserts, stony desert; 1300-5000 m.

568 **12.** *Artemisia chinensis* **(Table 1, Figs. 6c, 15)**

569 Pollen grains spheroidal or oblate. Almost circular in equatorial view and trilobate circular in polar view.

570 Apertures tricolporate. The exine near the colpi gradually thinned. P = 21.53 ± 1.95 μm, E = 22.75 ± 2.00 μm,

571 P/E = 0.95 ± 0.05, T = 2.97 ± 0.40 μm, L = 23.71 ± 2.30 μm, T/L = 0.13 ± 0.01. The exine ornamentation is

psilate (LM), spinulate (SEM). Under SEM, D = 0.70 ± 0.05 μm, H = 0.55 ± 0.07 μm, D/H = 1.29 ± 0.19, Gs = 0.27 ± 0.07 μm, Ss = 0.91 ± 0.17 μm, Gs/Ss = 0.31 ± 0.09.

Habitat: littoral plants found on raised coral outcrops.

13. *Artemisia kurramensis* (Table 1, Figs. 7a, 15)

Pollen grains spheroidal. Almost circular in equatorial view and trilobate circular in polar view. Apertures tricolporate. The exine near the colpi gradually thinned. P = 19.71 ± 1.28 μm, E = 19.35 ± 1.02 μm, P/E = 1.02 ± 0.05, T = 3.30 ± 0.38 μm, L = 19.44 ± 0.92 μm, T/L = 0.17 ± 0.02. The exine ornamentation is psilate (LM), spinulate (SEM). Under SEM, D = 0.38 ± 0.04 μm, H = 0.27 ± 0.03 μm, D/H = 1.41 ± 0.21, Gs = 0.23 ± 0.07 μm, Ss = 1.25 ± 0.21 μm, Gs/Ss = 0.19 ± 0.06.

Habitat: foothills, mountain slopes, dry graveyards, field borders with sparse vegetation on gravelly, fine to coarse sandy-clay soils.

14. *Artemisia compactum* (Table 1, Figs. 7b, 15)

Pollen grains spheroidal. Almost circular in equatorial view and trilobate circular in polar view. Apertures tricolporate. The exine near the colpi gradually thinned. P = 22.33 ± 1.81 μm, E = 21.97 ± 1.23 μm, P/E = 1.02 ± 0.06, T = 2.97 ± 0.43 μm, L = 21.67 ± 0.87 μm, T/L = 0.14 ± 0.02. The exine ornamentation is psilate (LM), spinulate (SEM). Under SEM, D = 0.41 ± 0.07 μm, H = 0.28 ± 0.03 μm, D/H = 1.50 ± 0.33, Gs = 0.51 ± 0.12 μm, Ss = 0.92 ± 0.12 μm, Gs/Ss = 0.56 ± 0.12.

Habitat: rocky slopes, semi-deserts, from low elevations to sub-alpine areas.

15. *Artemisia maritima* (Table 1, Figs. 7c, 15)

Pollen grains prolate. Almost circular in equatorial view and trilobate circular in polar view. Apertures tricolporate. The exine near the colpi gradually thinned. P = 26.24 ± 1.61 μm, E = 23.09 ± 1.43 μm, P/E = 1.14 ± 0.06, T = 3.54 ± 0.44 μm, L = 24.42 ± 1.51 μm, T/L = 0.14 ± 0.02. The exine ornamentation is psilate (LM), spinulate (SEM). Under SEM, D = 0.28 ± 0.04 μm, H = 0.23 ± 0.06 μm, D/H = 1.30 ± 0.34, Gs = 0.53 ± 0.12 μm, Ss = 1.08 ± 0.12 μm, Gs/Ss = 0.50 ± 0.13.

Habitat: saltmarsh, dry and calcareous hillsides, seashores, and dry saline or alkaline soils.

16. *Artemisia aralensis* (Table 1, Figs. 8a, 15)

Pollen grains prolate or spheroidal. Almost circular in equatorial view and trilobate circular in polar view. Apertures tricolporate. The exine near the colpi gradually thinned. P = 22.32 ± 1.72 μm, E = 21.91 ± 1.63 μm, P/E = 1.02 ± 0.06, T = 3.16 ± 0.36 μm, L = 22.76 ± 1.45 μm, T/L = 0.14 ± 0.01. The exine ornamentation is psilate (LM), spinulate (SEM). Under SEM, D = 0.25 ± 0.04 μm, H = 0.22 ± 0.04 μm, D/H = 1.16 ± 0.28, Gs = 0.50 ± 0.13 μm, Ss = 1.09 ± 0.18 μm, Gs/Ss = 0.46 ± 0.14.

603 Habitat: clayey, sandy loam, solonetzic soils.

17. *Artemisia annua* (Table 1, Figs. 8b, 15)

Pollen grains prolate or spheroidal. Almost circular in equatorial view and trilobate circular in polar view. Apertures tricolporate. The exine near the colpi gradually thinned. $P = 19.71 \pm 0.84$ μm, $E = 19.45 \pm 1.32$ μm, $P/E = 1.02 \pm 0.07$, $T = 3.45 \pm 0.25$ μm, $L = 19.20 \pm 0.92$ μm, $T/L = 0.18 \pm 0.01$. The exine ornamentation is psilate (LM), spinulate (SEM). Under SEM, $D = 0.45 \pm 0.06$ μm, $H = 0.39 \pm 0.05$ μm, $D/H = 1.18 \pm 0.25$, $Gs = 0.27 \pm 0.08$ μm, $Ss = 1.29 \pm 0.16$ μm, $Gs/Ss = 0.21 \pm 0.08$.

Habitat: hills, waysides, wastelands, outer forest margins, steppes, forest steppes, dry flood lands, terraces, semidesert steppes, rocky slopes, roadsides, saline soils; 2000-3700 m.

18. *Artemisia freyniana* (Table 1, Figs. 8c, 15)

Pollen grains prolate. Almost circular in equatorial view and trilobate circular in polar view. Apertures tricolporate. The exine near the colpi gradually thinned. $P = 23.39 \pm 1.21$ μm, $E = 21.30 \pm 1.07$ μm, $P/E = 1.10 \pm 0.04$, $T = 3.17 \pm 0.26$ μm, $L = 21.29 \pm 0.95$ μm, $T/L = 0.15 \pm 0.01$. The exine ornamentation is psilate (LM), spinulate (SEM). Under SEM, $D = 0.56 \pm 0.05$ μm, $H = 0.40 \pm 0.06$ μm, $D/H = 1.40 \pm 0.15$, $Gs = 0.20 \pm 0.05$ μm, $Ss = 1.15 \pm 0.15$ μm, $Gs/Ss = 0.18 \pm 0.05$.

Habitat: steppes, slopes, dry river valleys, riverbanks, outer forest margins.

19. *Artemisia stechmanniana* (Table 1, Figs. 9a, 15)

Pollen grains prolate or spheroidal. Almost circular in equatorial view and trilobate circular in polar view. Apertures tricolporate. The exine near the colpi gradually thinned. $P = 26.31 \pm 1.48$ μm, $E = 25.16 \pm 1.22$ μm, $P/E = 1.05 \pm 0.07$, $T = 3.97 \pm 0.60$ μm, $L = 23.45 \pm 1.38$ μm, $T/L = 0.17 \pm 0.02$. The exine ornamentation is psilate (LM), spinulate (SEM). Under SEM, $D = 0.37 \pm 0.05$ μm, $H = 0.35 \pm 0.05$ μm, $D/H = 1.07 \pm 0.25$, $Gs = 0.19 \pm 0.04$ μm, $Ss = 1.40 \pm 0.24$ μm, $Gs/Ss = 0.14 \pm 0.04$.

Habitat: hillsides, roadsides, shrubland, and forest-steppe areas, and often becoming the dominant species or main associated species of plant communities in some areas of mountainous sunny slopes.

20. *Artemisia pontica* (Table 1, Figs. 9b, 15)

Pollen grains prolate or spheroidal. Almost circular in equatorial view and trilobate circular in polar view. Apertures tricolporate. The exine near the colpi gradually thinned. $P = 20.64 \pm 1.54$ μm, $E = 19.62 \pm 1.59$ μm, $P/E = 1.05 \pm 0.07$, $T = 3.01 \pm 0.39$ μm, $L = 19.75 \pm 0.84$ μm, $T/L = 0.15 \pm 0.02$. The exine ornamentation is psilate (LM), spinulate (SEM). Under SEM, $D = 0.60 \pm 0.11$ μm, $H = 0.37 \pm 0.06$ μm, $D/H = 1.63 \pm 0.37$, $Gs = 0.17 \pm 0.04$ μm, $Ss = 1.32 \pm 0.27$ μm, $Gs/Ss = 0.13 \pm 0.04$.

Habitat: rocky slopes, dry valleys, steppes, hills; low to middle elevations.

21. *Artemisia frigida* (Table 1, Figs. 9c, 15)

Pollen grains prolate or spheroidal. Almost circular in equatorial view and trilobate circular in polar view. Apertures tricolporate. The exine near the colpi gradually thinned. P = 25.11 ± 1.75 μm, E = 24.90 ± 1.48 μm, P/E = 1.01 ± 0.07, T = 4.61 ± 0.74 μm, L = 24.83 ± 1.27 μm, T/L = 0.19 ± 0.02. The exine ornamentation is psilate (LM), spinulate (SEM). Under SEM, D = 0.46 ± 0.08 μm, H = 0.32 ± 0.04 μm, D/H = 1.44 ± 0.26, Gs = 0.31 ± 0.08 μm, Ss = 1.30 ± 0.18 μm, Gs/Ss = 0.24 ± 0.06.

Habitat: steppes, sub-alpine meadows, dry hillsides, stable dunes, dry waste areas; 1000-4000 m.

22. *Artemisia rupestris* (Table 1, Figs. 10a, 15)

Pollen grains prolate or spheroidal. Almost circular in equatorial view and trilobate circular in polar view. Apertures tricolporate. The exine near the colpi gradually thinned. P = 24.45 ± 1.41 μm, E = 22.92 ± 1.40 μm, P/E = 1.07 ± 0.08, T = 3.18 ± 0.40 μm, L = 21.96 ± 1.15 μm, T/L = 0.14 ± 0.02. The exine ornamentation is psilate (LM), spinulate (SEM). Under SEM, D = 0.55 ± 0.05 μm, H = 0.33 ± 0.04 μm, D/H = 1.68 ± 0.28, Gs = 0.25 ± 0.07 μm, Ss = 0.91 ± 0.11 μm, Gs/Ss = 0.28 ± 0.09.

Habitat: dry hills, desert or semidesert steppes, grassy marshlands, dry river valleys, riverbeds, scrub, forest margins.

23. *Artemisia sericea* (Table 1, Figs. 10b, 15)

Pollen grains spheroidal or oblate. Almost circular in equatorial view and trilobate circular in polar view. Apertures tricolporate. The exine near the colpi gradually thinned. P = 26.31 ± 1.31 μm, E = 27.90 ± 1.67 μm, P/E = 0.94 ± 0.03, T = 3.75 ± 0.32 μm, L = 26.89 ± 2.12 μm, T/L = 0.14 ± 0.01. The exine ornamentation is psilate (LM), spinulate (SEM). Under SEM, D = 0.89 ± 0.09 μm, H = 0.54 ± 0.10 μm, D/H = 1.71 ± 0.36, Gs = 0.28 ± 0.07 μm, Ss = 1.74 ± 0.31 μm, Gs/Ss = 0.16 ± 0.05.

Habitat: Forest margins, hills, steppes, canyons, waste areas.

24. *Artemisia absinthium* (Table 1, Figs. 10c, 15)

Pollen grains prolate. Almost circular in equatorial view and trilobate circular in polar view. Apertures tricolporate. The exine near the colpi gradually thinned. P = 22.79 ± 1.22 μm, E = 20.84 ± 1.11 μm, P/E = 1.09 ± 0.05, T = 3.39 ± 0.31 μm, L = 19.92 ± 1.74 μm, T/L = 0.17 ± 0.01. The exine ornamentation is psilate (LM), spinulate (SEM). Under SEM, D = 0.59 ± 0.05 μm, H = 0.40 ± 0.06 μm, D/H = 1.52 ± 0.25, Gs = 0.18 ± 0.04 μm, Ss = 1.11 ± 0.15 μm, Gs/Ss = 0.16 ± 0.04.

Habitat: hillsides, steppes, scrub, forest margins, often in locally moist situations; 1100-1500 m.

25. *Artemisia abrotanum* (Table 1, Figs. 11a, 15)

Pollen grains prolate or spheroidal. Almost circular in equatorial view and trilobate circular in polar view. Apertures tricolporate. The exine near the colpi gradually thinned. P = 24.47 ± 1.56 μm, E = 23.73 ± 1.65 μm, P/E = 1.03 ± 0.07, T = 3.15 ± 0.28 μm, L = 18.82 ± 0.81 μm, T/L = 0.17 ± 0.01. The exine ornamentation is psilate (LM), spinulate (SEM). Under SEM, D = 0.72 ± 0.10 μm, H = 0.51 ± 0.05 μm, D/H = 1.44 ± 0.25, Gs = 0.22 ± 0.04 μm, Ss = 1.41 ± 0.19 μm, Gs/Ss = 0.16 ± 0.04.

Habitat: the wasteland of western, southern, central, and southern Europe.

26. *Artemisia blepharolepis* (Table 1, Figs. 11b, 15)

Pollen grains spheroidal. Almost circular in equatorial view and trilobate circular in polar view. Apertures tricolporate. The exine near the colpi gradually thinned. P = 18.96 ± 0.98 μm, E = 19.26 ± 0.99 μm, P/E = 0.99 ± 0.05, T = 3.15 ± 0.28 μm, L = 18.82 ± 0.81 μm, T/L = 0.17 ± 0.01. The exine ornamentation is psilate (LM), spinulate (SEM). Under SEM, D = 0.69 ± 0.09 μm, H = 0.44 ± 0.07 μm, D/H = 1.64 ± 0.44, Gs = 0.37 ± 0.18 μm, Ss = 1.68 ± 0.20 μm, Gs/Ss = 0.23 ± 0.14.

Habitat: low-altitude areas of dry slopes, grasslands, steppes, waste areas, roadsides, dunes near riverbanks.

27. *Artemisia norvegica* (Table 1, Figs. 11c, 15)

Pollen grains prolate. Almost circular in equatorial view and trilobate circular in polar view. Apertures tricolporate. The exine near the colpi gradually thinned. P = 24.51 ± 1.40 μm, E = 22.11 ± 1.05 μm, P/E = 1.11 ± 0.06, T = 3.48 ± 0.39 μm, L = 22.61 ± 1.31 μm, T/L = 0.15 ± 0.01. The exine ornamentation is psilate (LM), spinulate (SEM). Under SEM, D = 0.67 ± 0.08 μm, H = 0.43 ± 0.11 μm, D/H = 1.66 ± 0.51, Gs = 0.19 ± 0.03 μm, Ss = 1.56 ± 0.24 μm, Gs/Ss = 0.12 ± 0.03.

Habitat: bare stony ground, Racomitrium heath, bouldery crests of solifluction terraces, and sometimes hollows between rocks.

28. *Artemisia tanacetifolia* (Table 1, Figs. 12a, 15)

Pollen grains prolate or spheroidal. Almost circular in equatorial view and trilobate circular in polar view. Apertures tricolporate. The exine near the colpi gradually thinned. P = 28.38 ± 0.90 μm, E = 27.75 ± 1.70 μm, P/E = 1.03 ± 0.06, T = 3.46 ± 0.47 μm, L = 27.63 ± 1.06 μm, T/L = 0.13 ± 0.02. The exine ornamentation is psilate (LM), spinulate (SEM). Under SEM, D = 0.71 ± 0.06 μm, H = 0.32 ± 0.04 μm, D/H = 2.23 ± 0.40, Gs = 0.30 ± 0.07 μm, Ss = 1.08 ± 0.16 μm, Gs/Ss = 0.29 ± 0.07.

Habitat: middle and low-altitude areas of forest grasslands, grasslands, meadows, forest edges, open forests, salty grasslands, grass slopes, and brushwood.

29. *Artemisia tournefortiana* (Table 1, Figs. 12b, 15)

Pollen grains prolate or spheroidal. Almost circular in equatorial view and trilobate circular in polar view. Apertures tricolporate. The exine near the colpi gradually thinned. P = 20.76 ± 0.98 μm, E = 20.43 ± 0.83 μm,

P/E = 1.02 ± 0.06, T = 3.33 ± 0.19 μm, L = 20.03 ± 0.79 μm, T/L = 0.17 ± 0.01. The exine ornamentation is psilate (LM), spinulate (SEM). Under SEM, D = 0.73 ± 0.06 μm, H = 0.42 ± 0.07 μm, D/H = 1.81 ± 0.33, Gs = 0.26 ± 0.07 μm, Ss = 1.25 ± 0.20 μm, Gs/Ss = 0.22 ± 0.08.

Habitat: widely distributed on hills, terraces, dry flood lands, waste fields, steppes, open forests, semi-marshlands.

30. *Artemisia dracunculus* (Table 1, Figs. 12c, 15)

Pollen grains spheroidal. Almost circular in equatorial view and trilobate circular in polar view. Apertures tricolporate. The exine near the colpi gradually thinned. P = 22.89 ± 1.24 μm, E = 22.87 ± 1.32 μm, P/E = 1.00 ± 0.05, T = 2.82 ± 0.52 μm, L = 21.91 ± 1.35 μm, T/L = 0.13 ± 0.03. The exine ornamentation is psilate (LM), spinulate (SEM). Under SEM, D = 0.68 ± 0.05 μm, H = 0.45 ± 0.07 μm, D/H = 1.56 ± 0.31, Gs = 0.31 ± 0.10 μm, Ss = 0.92 ± 0.15 μm, Gs/Ss = 0.34 ± 0.11.

Habitat: dry slopes, steppes, semidesert steppes, forest steppes, forest margins, waste areas, roadsides, terraces, subalpine meadows, meadow steppes, dry river valleys, rocky slopes, saline-alkaline soils; 500-3800 m.

31. *Artemisia japonica* (Table 1, Figs. 13a, 15)

Pollen grains spheroidal or oblate. Almost circular in equatorial view and trilobate circular in polar view. Apertures tricolporate. The exine near the colpi gradually thinned. P = 20.18 ± 1.28 μm, E = 21.23 ± 1.26 μm, P/E = 0.95 ± 0.05, T = 4.24 ± 0.49 μm, L = 21.02 ± 1.14 μm, T/L = 0.20 ± 0.02. The exine ornamentation is psilate (LM), spinulate (SEM). Under SEM, D = 0.57 ± 0.05 μm, H = 0.32 ± 0.05 μm, D/H = 1.80 ± 0.24, Gs = 0.26 ± 0.05 μm, Ss = 1.26 ± 0.16 μm, Gs/Ss = 0.21 ± 0.04.

Habitat: forest margins, waste areas, shrublands, hills, slopes, roadsides. Low elevations to 3300 m.

32. *Artemisia capillaris* (Table 1, Figs. 13b, 15)

Pollen grains spheroidal or oblate. Almost circular in equatorial view and trilobate circular in polar view. Apertures tricolporate. The exine near the colpi gradually thinned. P = 19.53 ± 1.09 μm, E = 19.64 ± 1.62 μm, P/E = 1.00 ± 0.08, T = 3.54 ± 0.34 μm, L = 19.18 ± 0.97 μm, T/L = 0.18 ± 0.01. The exine ornamentation is psilate (LM), spinulate (SEM). Under SEM, D = 0.51 ± 0.06 μm, H = 0.36 ± 0.04 μm, D/H = 1.44 ± 0.30, Gs = 0.26 ± 0.04 μm, Ss = 1.27 ± 0.16 μm, Gs/Ss = 0.21 ± 0.05.

Habitat: humid slopes, hills, terraces, roadsides, riverbanks; 100-2700 m.

33. *Artemisia campestris* (Table 1, Figs. 13c, 15)

Pollen grains prolate or spheroidal. Almost circular in equatorial view and trilobate circular in polar view. Apertures tricolporate. The exine near the colpi gradually thinned. P = 21.69 ± 0.85 μm, E = 21.26 ± 0.89 μm, P/E = 1.02 ± 0.07, T = 3.68 ± 0.33 μm, L = 21.21 ± 0.89 μm, T/L = 0.17 ± 0.02. The exine ornamentation is

727 psilate (LM), spinulate (SEM). Under SEM, D = 0.57 ± 0.09 μm, H = 0.38 ± 0.05 μm, D/H = 1.53 ± 0.23, Gs
728 = 0.41 ± 0.09 μm, Ss = 1.23 ± 0.19 μm, Gs/Ss = 0.34 ± 0.08.

729 Habitat: steppes, waste areas, rocky slopes, dune margins; 300-3100 m.

34. *Kaschgaria brachanthemoides* (Table 1, Figs. 14a, 15)

731 Pollen grains prolate or spheroidal. Almost circular in equatorial view and trilobate circular in polar view.
732 Apertures tricolporate. The exine near the colpi gradually thinned. P = 23.26 ± 1.44 μm, E = 22.09 ± 1.18 μm,
733 P/E = 1.06 ± 0.08, T = 3.93 ± 0.44 μm, L = 21.01 ± 1.28 μm, T/L = 0.19 ± 0.02. The exine ornamentation is
734 psilate (LM), spinulate (SEM). Under SEM, D = 0.55 ± 0.07 μm, H = 0.44 ± 0.05 μm, D/H = 1.25 ± 0.20, Gs
735 = 0 μm, Ss = 1.75 ± 0.20 μm, Gs/Ss = 0, Pertorations spacing (Ps) = 0.47 ± 0.14 μm.

736 Habitat: dry mountain valleys, old dry riverbeds; 1000-1500 m.

35. *Ajania pallasiana* (Table 1, Figs. 14b, 15)

738 Pollen grains spheroidal. Almost circular in equatorial view and trilobate circular in polar view. Apertures
739 tricolporate. The exine near the colpi gradually thinned. P = 35.16 ± 2.68 μm, E = 35.92 ± 3.31 μm, P/E = 0.98
740 ± 0.03, T = 10.23 ± 0.85 μm, L = 38.31 ± 2.06 μm, T/L = 0.27 ± 0.03 μm. The exine ornamentation spinose.
741 Under SEM, D = 4.41 ± 0.35 μm, H = 3.47 ± 0.38 μm, D/H = 1.29 ± 0.21, Gs = 0 μm, Ss = 7.84 ± 1.25 μm,
742 Gs/Ss = 0, Ps = 0.39 ± 0.12 μm.

743 Habitat: thickets, mountain slopes, 200-2900 m.

36. *Chrysanthemum indicum* (Table 1, Figs. 14c, 15)

745 Pollen grains prolate or spheroidal or oblate. Almost circular in equatorial view and trilobate circular in polar
746 view. Apertures tricolporate. The exine near the colpi gradually thinned. P = 33.54 ± 1.71 μm, E = 34.42 ±
747 2.46 μm, P/E = 0.98 ± 0.08, T = 8.65 ± 0.89 μm, L = 34.82 ± 1.65 μm, T/L = 0.25 ± 0.02. The exine
748 ornamentation spinose. Under SEM, D = 2.94 ± 0.33 μm, H = 3.59 ± 0.29 μm, D/H = 0.82 ± 0.10, Gs = 0 μm,
749 Ss = 7.11 ± 0.76 μm, Gs/Ss = 0, Ps = 0.37 ± 0.13 μm.

750 Habitat: grasslands on mountain slopes, thickets, wet places by rivers, fields, roadsides, saline places by
751 seashores, under shrubs, 100-2900 m.

752 **Appendix B**

753 **Table B1.** List of the voucher specimen in PE Herbarium, Institute of Botany, Chinese Academy of Sciences

Subgenus	Species	Specimen barcodes	Coll. No.	Habitat photograph sources
Subg. *Tridentata*	*Artemisia cana*	PE 01668975	H.Mozingo 79-97	© Jason Headley https://www.inaturalist.org/photos/54492753
	Artemisia tridentata	PE 01917565	Debreczy-Racz-Biro s.n.	© Matt Berger https://www.inaturalist.org/photos/117436654
	Artemisia californica	PE 01668942	Lewis S.Rose 69107	© Don Rideout https://www.inaturalist.org/photos/108921528
Subg. *Artemisia*, Sect. *Artemisia*	*Artemisia indica*	PE 00444597	Tian-Lun Dai 104336	© yangting https://www.inaturalist.org/photos/66336449
	Artemisia argyi	PE 00420930	K.M.Liou 9276	© sergeyprokopenko https://www.inaturalist.org/photos/95820686
	Artemisia mongolica	PE 00445665	Cheng-Yuan Yang & Zu-Gui Li 36466a	© Nikolay V Dorofeev https://www.inaturalist.org/photos/163584035
	Artemisia vulgaris	PE 01669703	P.Frost-Olsen 1833	© Sara Rall https://www.inaturalist.org/photos/120600448
	Artemisia selengensis	PE 00479106	Ming-Gang Li et al. 486	© Gularjanz Grigoryi Mihajlovich https://www.inaturalist.org/photos/46352423
	Artemisia ludoviciana	PE 01669278	W.Hess 2405	© Ethan Rose https://www.inaturalist.org/photos/77690333
	Artemisia roxburghiana	PE 00478222	Xingan collection team 70	© Bo-Han Jiao
	Artemisia rutifolia	PE 00478427	Ke Guo 12528	© Daba https://www.inaturalist.org/photos/62207191
Subg. *Pacifica*	*Artemisia chinensis*	PE 01565620	Y.Tateishi J.Murata.Y.Endo et al. 15202	© Jia-Hao Shen

Subg. *Seriphidium*	*Artemisia kurramensis*	PE 01669178	M.Togasi 1672	© Andrey Vlasenko https://www.inaturalist.org/photos/133758174
	Artemisia compactum	PE 00457459	Hexi team 313	© Chen Chen
	Artemisia maritima	No. 1338063	s.n.	© torkild https://www.inaturalist.org/photos/86515371
	Artemisia aralensis	No. 202006	s.n.	© Полынь аральская https://www.plantarium.ru/lang/en/page/image/id/73063.html
	Artemisia annua	PE 01197344	Wen-Hong Jin-Tian, Kai-Yong Lang, Ge Yang 328	© Chen Chen
Subg. *Artemisia*, Sect. *Abrotanum* I	*Artemisia freyniana*	PE 01669030	S.Kharkevich 753	© Шильников Дмитрий Сергеевич https://www.inaturalist.org/photos/154390279
	Artemisia stechmanniana	PE 00478480	Shen-E Liu, Pei-Yun Fu et al. 4715	© Bo-Han Jiao
	Artemisia pontica	PE 01589110	Gy.Szollat & K.Dobolyi s.n.	© Martin Pražák https://www.inaturalist.org/photos/93438780
Subg. *Absinthium*	*Artemisia frigida*	PE 00444197	Ren-Chang Qin 0913	© Suzanne Dingwell https://www.inaturalist.org/photos/125022240
	Artemisia rupestris	PE 00478380	Anonymous 948	© Bo-Han Jiao
	Artemisia sericea	PE 01669585	N.Maltzev 3175	© svetlana_katana https://www.inaturalist.org/photos/48033353
	Artemisia absinthium	PE 01668816	G.Bujorean s.n.	© Станислав Лебедев https://www.inaturalist.org/photos/123569286
Subg. *Artemisia*, Sect. *Abrotanum* II	*Artemisia abrotanum*	PE 01668792	T.Leonova s.n.	© Андрей Москвичев https://www.inaturalist.org/photos/116106722
	Artemisia blepharolepis	PE 00421006	Kun-Jun Fu 7252	© Ji-Ye Zheng
Subg. *Artemisia*, Sect. *Abrotanum* III	*Artemisia norvegica*	PE 01669339	J.Haug s.n.	© Erin Springinotic https://www.inaturalist.org/photos/161393521

	Artemisia tanacetifolia	PE 00479744	T.P.Wang W.3379	© Alexander Dubynin https://www.inaturalist.org/photos/78902853
	Artemisia tournefortiana	PE 00479786	Ren-Chang Qin 2266	© Chen Chen
Subg. ***Dracunculus***	*Artemisia dracunculus*	PE 00421462	Shen-E Liu et al. 8084	© anatolymikhaltsov https://www.inaturalist.org/photos/76312868
	Artemisia japonica	PE 00444874	Qianbei team 2850	© 陳達智 https://www.inaturalist.org/photos/44507659
	Artemisia capillaris	PE 00421156	Han-Chen Wang 4078	© Cheng-Tao Lin https://www.inaturalist.org/photos/60639286
	Artemisia campestris	PE 00421097	T.N.Liou L.1008	© pedrosanz-anapri https://www.inaturalist.org/photos/113822257
Outgroups	*Kaschagaria brachanthemoides*	PE 01577564	Yun-Wen Tian 22158	© Chen Chen
	Ajania pallasiana	PE 00420032	Guang-Zheng Wang 497	© Игорь Поспелов https://www.inaturalist.org/photos/162408714
	Chrysanthemum indicum	PE 01258852	Anonymous 221	© Bo-Han Jiao

754 Note: In the absence of habitat photographs of two species, habitat photographs of species with which they have close
755 phylogenetic relationships and similar habitats were used in this study instead, i.e. the habitat photograph of *Kaschagaria*
756 *komarovii* was used instead of *Kaschagaria brachanthemoides,* the habitat photograph of *Artemisia taurica* for *Artemisia*
757 *kurramensis*.

758 **Table B12.** List of the voucher specimens in PE Herbarium, Institute of Botany, Chinese Academy of
759 Sciences. Sample No. 0 was the ~~sample~~ specimen ~~in the original text~~ for cluster analysis.~~,~~ Sample Nos.1-4
760 were used in testing intraspecific variability in pollen exine ultrastructure characters among three
761 representative species.~~the newly added voucher specimen in this response.~~

Sample No.	SWS type		LNS type		SG type	
	Artemisia vulgaris		*Artemisia annua*		*Artemisia maritima*	
	Specimen barcodes	Coll. No.	Specimen barcodes	Coll. No.	Specimen No.	Coll. No.
0	PE 01669703	P.Frost-Olsen 1833	PE 01197344	Wen-Hong Jin-Tian, Kai-Yong Lang, Ge Yang 328	No. 1338063	s.n.
1	PE 00532417	75-1521	PE 420433	Xue-Zhong Liang 328	No. 209452	G. Belloteau 1912.9.25
2	PE 00492025	K.M.Liou L.6601	PE 420647	T.N.Liou & C.Wang 731	No. 209446	s.n.
3	PE 00492038	P.C.Hoch, Jia-Rui Chen 86077	PE 420660	Da-Shun Wang 856	s.n.	Hanelt Schultze-Motel 446
4	PE 00492029	Hong-Bin Cui, You-Run Lin, Zhen-Dai Xia 80-290	PE 420664	Lei,C.I. 858	s.n.	O. Nordstedt 1901-10-9

762

Author contributions. YFW, YFY, TGG conceived the ideas, LLL, BHJ, KQL, and BS collected the literature, LLL extracted and compiled the data, LLL, FQ, and BHJ made the statistical analysis, GX and ML collected pictures, LLL, KQL, and BS drew the figures and tables, LLL, YFW, YFY, LJF, FQ, and GX wrote the first draft of this manuscript, DKF corrected the various versions of the manuscript, while all authors contributed substantially to revisions.

Competing interests. The authors declare that they have no conflict of interest.

Acknowledgments. We thank Dr. Jian Yang, Institute of Botany, Chinese Academy of Sciences, for his kind help in drafting graphics. We appreciate Chen Chen from Institute of Botany, Chinese Academy of Sciences, Ji-Ye Zheng from No. 1 Middle School of Jiyang Shandong, and Jia-Hao Shen from Institute of Botany, Jiangsu Province and Chinese Academy of Sciences (Nanjing Botanical Garden Mem. Sun Yat-Sen), for their enthusiastic assistance in providing habitat photographs.

Financial support. This research was supported by the Strategic Priority Research Program of the Chinese Academy of Sciences (No. XDB26000000), National Natural Science Foundation of China (Nos. 31970223, 32070240, and 42077416), and the Chinese Academy of Sciences President's International Fellowship Initiative (No. 2018VBA0016).

References

Beerling, D. J. and Royer, D. L.: Convergent Cenozoic CO_2 history, Nat. Geosci., 4, 418-420, https:// 10.1038/ngeo1186, 2011.

Bhattacharya, T., Tierney, J. E., Addison, J. A., and Murray, J. W.: Ice-sheet modulation of deglacial North American monsoon intensification, Nat. Geosci., 11, 848-852, https://doi.org/10.1038/s41561-018-0220-7, 2018.

Blackmore, S., Wortley, A. H., Skvarla, J. J., and Robinson, H., V. A. Funk, A. Susanna, Stuessy, T. F., and Bayer, R. J. (Eds.): Evolution of pollen in Compositae. In Systematics, Evolution and Biogeography of the Compositae, International Association of Plant Taxonomy, Vienna, 2009.

Bremer, K. and Humphries, C. J.: Generic monograph of the Asteraceae-Anthemideae, Bull. Nat. Hist. Mus., 23, 71-177, https://www.biodiversitylibrary.org/item/19562, 1993.

Brummitt, N., Araujo, A. C., and Harris, T.: Areas of plant diversity-What do we know?, Plants people planet, 3, 33-44, https://doi.org/10.1002/ppp3.10110, 2021.

Cai, M., Ye, P., Yang, X., and Li, C.: Vegetation and climate change in the Hetao Basin (Northern China) during the last interglacial-glacial cycle, J. Asian Earth Sci., 171, 1-8, https://doi.org/10.1016/j.jseaes.2018.11.024, 2019.

Cao, X. Y., Tian, F., Li, K., Ni, J., Yu, X. S., Liu, L. N., and Wang, N. N.: Lake surface sediment pollen dataset for the alpine meadow vegetation type from the eastern Tibetan Plateau and its potential in past climate reconstructions, Earth Syst. Sci. Data, 13, 3525-3537, https://doi.org/10.5194/essd-13-3525-2021, 2021.

Chen, J. X., Shi, X. F., Liu, Y. G., Qiao, S. Q., Yang, S. X., Yan, S. J., Lv, H. H., Li, J. Y., Li, X. Y., and Li, C. X.: Holocene vegetation dynamics in response to climate change and hydrological processes in the Bohai region, Clim. Past., 16, 2509-2531, https://doi.org/10.5194/cp-16-2509-2020, 2020.

Chen, S. B.: Pollen Morphology of *Artemisia* L. from China: A Discussion on the Relationship between Pollen Morphology of *Artemisia* L. and Allies, 1987 (in Chinese).

Chen, S. B. and Zhang, J. T.: A Study on Pollen Morphology of Some Chinese Genera in Tribe Anthemideae, Acta Phytotax. Sin., 29, 246-251, 1991 (in Chinese).

China Vegetation Editorial Committee, Wu, Z. Y. (Ed.): Chinese Vegetation Science Press, Beijing, 1980 (in Chinese).

Cui, Q. Y., Zhao, Y., Qin, F., Liang, C., Li, Q., and Geng, R. W.: Characteristics of the modern pollen assemblages from different vegetation zones in Northeast China: Implications for pollen-based climate reconstruction, Sci. China-Earth Sci., 62, 1564-1577, https://doi.org/10.1007/s11430-018-9386-9, 2019.

Davies, C. P. and Fall, P. L.: Modern pollen precipitation from an elevational transect in central Jordan and its relationship to vegetation, J. Biogeogr., 28, 1195-1210, https://doi.org/10.1046/j.1365-2699.2001.00630.x, 2001.

El-Moslimany, A. P.: Ecological significance of common nonarboreal pollen : examples from drylands of the Middle East, Rev. Palaeobot. Palynol., 64, 343-350, https://doi.org/10.1016/0034-6667(90)90150-h, 1990.

Erdtman, G.: The acetolysis method, a revised descriptions, Svensk Botanisk Tidskrift, 54, 561-564, 1960.

Ferguson, D. K., Zetter, R., and Paudayal, K. N.: The need for the SEM in palaeopalynology, C. R. Palevol, 6, 423-430, http://doi.org/10.1016/j.crpv.2007.09.018, 2007.

813 Ghahraman, A., Nourbakhsh, N., Mehdi, G. K., and Atar, F.: Pollen Morphology of *Artemisia* L. (Asteraceae) in Iran,
814   Iran. Journ. Bot., 13, 21-29, 2007.

815 GBIF. org GBIF Occurrence Download: https://doi.org/10.15468/dl.596xd9, last access: 09 November 2021.

816 Grímsson, F., Zetter, R., and Hofmann, C.: *Lythrum* and *Peplis* from the Late Cretaceous and Cenozoic of North America
817   and Eurasia: new evidence suggesting early diversification within the Lythraceae, Am. J. Bot., 98, 1801-1815,
818   https://doi.org/10.3732/ajb.1100204, 2011.

819 Grímsson, F., Zetter, R., and Leng, Q.: Diverse fossil Onagraceae pollen from a Miocene palynoflora of north-east China:
820   early steps in resolving the phytogeographic history of the family, Plant Syst. Evol., 298, 671-687,
821   https://doi.org/10.1007/s00606-011-0578-0, 2012.

822 Guiot, J. and Cramer, W.: Climate change: The 2015 Paris Agreement thresholds and Mediterranean basin ecosystems,
823   Science, 354, 465-468, https://doi.org/10.1126/science.aah5015, 2016.

824 Halbritter, H., Silvia, U., Grímsson, F., Weber, M., Zetter, R., Hesse, M., Buchner, R., Svojtka, M., and Frosch-Radivo, A.:
825   Illustrated Pollen Terminology, Springer Open, 2018.

826 Hayat, M. Q., Ashraf, M., Khan, M. A., Yasmin, G., and Jabeen, S.: Palynological study of the genus *Artemisia*
827   (Asteraceae) and its systematic implications, Pak. J. Bot., 42, 751-763, https://doi.org/10.1094/MPMI-23-4-0522,
828   2010.

829 Hayat, M. Q., Ashraf, M., Khan, M. A., Yasmin, G., Shaheen, N., and Jabeen, S.: Phylogenetic analysis of *Artemisia* L.
830   (Asteraceae) based on micromorphological traits of pollen grains, Afr. J. Biotechnol., 8, 6561-6568,
831   https://doi.org/10.1556/AMicr.56.2009.4.11, 2009.

832 Herzschuh, U., Tarasov, P., Wünnemann, B., and Kai, H.: Holocene vegetation and climate of the Alashan Plateau, NW
833   China, reconstructed from pollen data, Paleogeogr. Paleoclimatol. Paleoecol., 211, 1-17,
834   https://doi.org/10.1016/j.palaeo.2004.04.001, 2004.

835 Hesse, M., Buchner, R., Froschradivo, A., Halbritter, H., Ulrich, S., Weber, M., and Zetter, R.: Pollen Terminology : An
836   illustrated handbook, Springer, NewYork, 2009.

837 Hussain, A., Potter, D., Hayat, M. Q., Sahreen, S., and Bokhari, S. A. I.: Pollen morphology and its systematic
838   implication on some species of *Artemisia* L. from Gilgit-Baltistan Pakistan, Bangladesh J. Plant Taxon., 26, 157-168,
839   https://doi.org/10.3329/bjpt.v26i2.44576, 2019.

840 Jiang, L., Q., W., Ye, L. Z., and R., L. Y.: Pollen Morphology of *Artemisia* L. and Its Systematic Significance, Wuhan
841   Univ. J. Nat. Sci., 10, 448-454, https://doi.org/10.1007/BF02830685, 2005.

842 Koutsodendris, A., Allstadt, F. J., Kern, O. A., Kousis, I., Schwarz, F., Vannacci, M., Woutersen, A., Appel, E., Berke, M.
843   A., Fang, X. M., Friedrich, O., Hoorn, C., Salzmann, U., and Pross, J.: Late Pliocene vegetation turnover on the NE
844   Tibetan Plateau (Central Asia) triggered by early Northern Hemisphere glaciation, Glob. Planet. Change, 180,
845   117-125, https://doi.org/10.1016/j.gloplacha.2019.06.001, 2019.

846 Li, F., Sun, J., Zhao, Y., Guo, X., Zhao, W., and Zhang, K.: Ecological significance of common pollen ratios: A review,
847   Front. Earth Sci. China, 4, 253-258, https://doi.org/10.1007/s11707-010-0112-7, 2010.

Li, X. L., Hao, Q. Z., Wei, M. J., Andreev, A. A., Wang, J. P., Tian, Y. Y., Li, X. L., Cai, M. T., Hu, J. M., and Shi, W.: Phased uplift of the northeastern Tibetan Plateau inferred from a pollen record from Yinchuan Basin, northwestern China, Sci. Rep., 7, 10, https://doi.org/10.1038/s41598-017-16915-z, 2017.

Ling, Y. R.: On the system of the genus *Artemisia* Linn. and the relationship with allies, Bulletin of Botanical Research, 2, 1-60, 1982 (in Chinese).

Ling, Y. R., Humphries, C. J., and Gilbert, M. G.: Flora of China, The Genus *Artemisia* L., Science Press, Beijing, 2011.

Liu, H. Y., Wang, Y., Tian, Y. H., Zhu, J. L., and Wang, H. Y.: Climatic and anthropogenic control of surface pollen assemblages in East Asian steppes, Rev. Palaeobot. Palynol., 138, 281-289, https://doi.org/10.1016/j.revpalbo.2006.01.008, 2006.

Lu, K. Q., Qin, F., Li, Y., Xie, G., Li, J. F., Cui, Y. M., Ferguson, D. K., Yao, Y. F., Wang, G. H., and Wang, Y. F.: A new approach to interpret vegetation and ecosystem changes through time by establishing a correlation between surface pollen and vegetation types in the eastern central Asian desert, Paleogeogr. Paleoclimatol. Paleoecol., 551, 12, https://doi.org/10.1016/j.palaeo.2020.109762, 2020.

Lu, L. L, Jiao, B. H., Qin, F., Xie, G., Lu, K. Q., Li, J. F., Sun, B., Li, M., Ferguson, D. K., Gao, T. G., Yao, Y. F., and Wang, Y. F.: *Artemisia* pollen dataset for exploring the potential ecological indicators in deep time, Zenodo [data set], https://doi.org//zenodo.69003086791891, 2022.

Ma, Q. F., Zhu, L. P., Wang, J. B., Ju, J. T., Lu, X. M., Wang, Y., Guo, Y., Yang, R. M., Kasper, T., Haberzettl, T., and Tang, L. Y.: *Artemisia*/Chenopodiaceae ratio from surface lake sediments on the central and western Tibetan Plateau and its application, Paleogeogr. Paleoclimatol. Paleoecol., 479, 138-145, https://doi.org/10.1016/j.palaeo.2017.05.002, 2017.

Malik, S., Vitales, D., Hayat, M. Q., Korobkov, A. A., Garnatje, T., and Valles, J.: Phylogeny and biogeography of *Artemisia* subgenus *Seriphidium* (Asteraceae: Anthemideae), Taxon, 66, 934-952, https://doi.org/10.12705/664.8, 2017.

Marsicek, J., Shuman, B. N., Bartlein, P. J., Shafer, S. L., and Brewer, S.: Reconciling divergent trends and millennial variations in Holocene temperatures, Nature, 554, 92-96, https://doi.org/10.1038/nature25464, 2018.

Martín, J., Torrell, M., and Valles, J.: Palynological features as a systematic marker in *Artemisia* L. and related genera (Asteraceae, Anthemideae), Plant Biol., 3, 372-378, https://doi.org/10.1055/s-2001-16462, 2001.

Martín, J., Torrell, M., Korobkov, A. A., and Valles, J.: Palynological features as a systematic marker in *Artemisia* L. and related genera (Asteraceae, Anthemideae) - II: Implications for subtribe Artemisiinae delimitation, Plant Biol., 5, 85-93, https://doi.org/10.1055/s-2001-16462, 2003.

McClelland, H. L. O., Halevy, I., Wolf-Gladrow, D. A., Evans, D., and Bradley, A. S.: Statistical Uncertainty in Paleoclimate Proxy Reconstructions, Geophys. Res. Lett., 48, e2021GL092773, https://doi.org/10.1029/2021GL092773, 2021.

Miao, Y. F., Meng, Q. Q., Fang, X. M., Yan, X. L., Wu, F. L., and Song, C. H.: Origin and development of *Artemisia* (Asteraceae) in Asia and its implications for the uplift history of the Tibetan Plateau: A review, Quatern. Int., 236, 3-12, https://doi.org/10.1016/j.quaint.2010.08.014, 2011.

Mo, R. G., Bai, X. L., Ma, y. Q., and Cao, R.: On the Intraspecific Variations of Pollen Morphology and Pollen Geography of a Relic Species-*Helianthemum songaricum* Schrenk, Acta Bot. Bor-Occid. Sin., 17, 528-532, 1997 (in Chinese).

Moberg, A., Sonechkin, D. M., Holmgren, K., Datsenko, N. M., and Karlen, W.: Highly variable Northern Hemisphere temperatures reconstructed from low- and high-resolution proxy data, Nature, 433, 613-617, https://doi.org/10.1038/nature03265, 2005.

Mosbrugger, V., Utescher, T., and L, D. D.: Cenozoic continental climatic evolution of Central Europe, Proc. Natl. Acad. Sci. U. S. A., 102, 14964-14969, https://doi.org/10.1073/pnas.0505267102, 2005.

Olson, D. M., Dinerstein, E., Wikramanayake, E. D., Burgess, N. D., Powell, G. V. N., Underwood, E. C., D'Amico, J. A., Itoua, I., Strand, H. E., Morrison, J. C., Loucks, C. J., Allnutt, T. F., Ricketts, T. H., Kura, Y., Lamoreux, J. F., Wettengel, W. W., Hedao, P., and Kassem, K. R.: Terrestrial ecoregions of the worlds: A new map of life on Earth, Bioscience, 51, 933-938, https://doi.org/10.1641/0006-3568(2001)051[0933:teotwa]2.0.co;2, 2001.

Sánchez-Murillo, R., Durán-Quesada, A. M., Esquivel-Hernández, G., Rojas-Cantillano, D., and Cobb, K. M.: Deciphering key processes controlling rainfall isotopic variability during extreme tropical cyclones, Nat. Commun., 10, 4321, https://doi.org/10.1038/s41467-019-12062-3, 2019.

Sanz, M., Vilatersana, R., Hidalgo, O., Garcia-Jacas, N., Susanna, A., Schneeweiss, G. M., and Vallès, J.: Molecular phylogeny and evolution of floral characters of *Artemisia* and allies (Anthemideae, Asteraceae): Evidence from nrDNA ETS and ITS sequences, Taxon, 57, 66-78, https://doi.org/10.2307/25065949, 2008.

Shan, B. Q., He, X. L., and Chen, Y. S.: Pollen Morphology of *Artemisia* in the Loess Plateau, Acta Botanica Boreali-Occidentalia Sinica, 27, 1373-1379, 2007 (in Chinese).

Sing, G. and Joshi, R. D.: Pollen Morphology of Some Eurasian Species of *Artemisia*, Grana Palynologica, 9, 50-62, https://doi.org/10.1080/00173136909436424, 1969.

Stix, E.: Pollenmorphologische Untersuchungen an Compositen, Grana, 2, 41-104, https://doi.org/10.1080/00173136009429443, 1960.

Sun, J. T. and Xu, Y. T.: Pollen morphology and its taxonomic significance of *Artemisia* Linn. from Shandong, Journal of Shandong Normal University, 12, 186-190, 1997 (in Chinese).

Sun, X. J., Du, N. Q., Weng, C. Y., Lin, R. F., and Wei, K. Q.: Paleovegetation and paleoenvironment of Manasi Lake, Xinjiang, N. W. China during the last 14000 years, Quaternary Sciences, 14, 239-248, 1994 (in Chinese).

Sun, X. J., Wang, F. Y., and Song, C. Q.: Pollen-climate response surfaces of selected taxa from northern China, Sci. China Ser. D-Earth Sci., 39, 486-493, 1996.

Tarasov, P. E., Cheddadi, R., Guiot, J., Bottema, S., Peyron, O., Belmonte, J., Ruiz-Sanchez, V., And, F. S., and Brewer, S.: A method to determine warm and cool steppe biomes from pollen data; application to the Mediterranean and Kazakhstan regions, J. Quat. Sci., 13, 335-344, https://doi.org/10.1002/(SICI)1099-1417(199807/08)13:4<335::AID-JQS375>3.0, 1998.

Tierney, J. E., Poulsen, C. J., Montanez, I. P., Bhattacharya, T., Feng, R., Ford, H. L., Honisch, B., Inglis, G. N., Petersen, S. V., Sagoo, N., Tabor, C. R., Thirumalai, K., Zhu, J., Burls, N. J., Foster, G. L., Godderis, Y., Huber, B. T., Ivany, L. C., Turner, S. K., Lunt, D. J., McElwain, J. C., Mills, B. J. W., Otto-Bliesner, B. L., Ridgwell, A., and Zhang, Y. G.: Past climates inform our future, Science, 370, eaay3701, https://doi.org/10.1126/science.aay3701, 2020.

922 Tutin, T. G., Persson, K., and Gutermann, W.: *Artemisia*, Flora Europaea 4, Cambridge University Press, Cambridge,
923   178-186, 1976.

924 Vallès, J., Garcia, S., Hidalgo, O., Martín, J., and Garnatje, T.: Biology, Genome Evolution, Biotechnological Issues and
925   Research Including Applied Perspectives in *Artemisia* (Asteraceae), Adv. Bot. Res., 60, 349-419, 2011.

926 Vrba, E. S.: Evolution, species and fossils-how does life evolve?, S. Afr. J. Sci., 76, 61-84, 1980.

927 Wang, F. X., Qian, N. F., Zhang, Y. L., and Yang, H. Q.: Pollen Morphology of Chinese Plants (2nd edition), Science
928   Press, Beijing, 1995 (in Chinese).

929 Wang, W. M.: On the origin and development of *Artemisia* (Asteraceae) in the geological past, Bot. J. Linnean Soc., 145,
930   331-336, https://doi.org/10.1111/j.1095-8339.2004.00287.x, 2004.

931 Wang, Y., Wang, W., Liu, L. N., Jiang, Y. J., Niu, Z. M., Ma, Y. Z., He, J., and Mensing, S. A.: Reliability of the
932   *Artemisia*/Chenopodiaceae pollen ratio in differentiating vegetation and reflecting moisture in arid and semi-arid
933   China, Holocene, 30, 858-864, https://doi.org/10.1177/0959683620902219, 2020.

934 Weng, C. Y., Sun, X. J., and Chen, Y. S.: Numerical characteristics of pollen assemblages of surface samples from the
935   West Kunlun mountains, Acta Botanica Sinica, 35, 69-79, 1993 (in Chinese).

936 Wodehouse, R. P.: Pollen Grain Morphology in the Classification of the Anthemideae, Bull. Torrey Bot. Club, 53,
937   479-485, https://doi.org/10.2307/2480028, 1926.

938 Wu, F. L., Fang, X. M., and Miao, Y. F.: Aridification history of the West Kunlun Mountains since the mid-Pleistocene
939   based on sporopollen and microcharcoal records, Paleogeogr. Paleoclimatol. Paleoecol., 547, 109680,
940   https://doi.org/10.1016/j.palaeo.2020.109680, 2020.

941 Xu, Q. H., Li, Y. C., Yang, X. L., and Zheng, Z. H.: Quantitative relationship between pollen and vegetation in northern
942   China, Sci. China Ser. D-Earth Sci., 50, 582-599, https://doi.org/10.1007/s11430-007-2044-y, 2007.

943 Yang, J., Spicer, R. A., Spicer, T. E. V., Arens, N. C., Jacques, F. M. B., Su, T., Kennedy, E. M., Herman, A. B., Steart, D.
944   C., Srivastava, G., Mehrotra, R. C., Valdes, P. J., Mehrotra, N. C., Zhou, Z. K., and Lai, J. S.: Leaf form-climate
945   relationships on the global stage: an ensemble of characters, Glob. Ecol. Biogeogr., 24, 1113-1125,
946   https://doi.org/10.1111/geb.12334, 2015.

947 Yi, S., Saito, Y., Zhao, Q. H., and Wang, P. X.: Vegetation and climate changes in the Changjiang (Yangtze River) Delta,
948   China, during the past 13,000 years inferred from pollen records, Quat. Sci. Rev., 22, 1501-1519,
949   https://doi.org/10.1016/s0277-3791(03)00080-5, 2003a.

950 Yi, S., Saito, Y., Oshima, H., Zhou, Y. Q., and Wei, H. L.: Holocene environmental history inferred from pollen
951   assemblages in the Huanghe (Yellow River) delta, China: climatic change and human impact, Quat. Sci. Rev., 22,
952   609-628, https://doi.org/10.1016/s0277-3791(02)00086-0, 2003b.

953 Zachos, J., Pagani, M., Sloan, L., Thomas, E., and Billups, K.: Trends, Rhythms, and Aberrations in Global Climate 65
954   Ma to Present, Science, 292, 686-693, https://doi.org/10.1126/science.1059412, 2001.

955 Zachos, J. C., Dickens, G. R., and Zeebe, R. E.: An early Cenozoic perspective on greenhouse warming and carbon-cycle
956   dynamics, Nature, 451, 279-283, https://doi.org/10.1038/nature06588, 2008.

957 Zhang, Y. N. and Qian, C.: SEM observation on pollen morphology of lily species, Acta Pratac. Sin., 20,
958   111-118, 2011 (in Chinese).

Zhang, X. S.: Vegetation map of China and its geographic pattern: Illustration of the vegetation map of the People's Republic of China (1:1 000 000), Geological Press, Beijing, 2007 (in Chinese).

Zhang, Y., Kong, Z. C., Wang, G. H., and Ni, J.: Anthropogenic and climatic impacts on surface pollen assemblages along a precipitation gradient in north-eastern China, Glob. Ecol. Biogeogr., 19, 621-631, https://doi.org/10.1111/j.1466-8238.2010.00534.x, 2010.

Zhao, X. L. and Yao, C. H.: Pollen Morphlogy Differences among *Osmanthus fragrans* Cultivars, J. Hubei Minzu Univ. (Nat. Sci. Ed.), 17, 16-20, 1999 (in Chinese).

Zhao, Y., Xu, Q. H., Huang, X. Z., Guo, X. L., and Tao, S. C.: Differences of modern pollen assemblages from lake sediments and surface soils in arid and semi-arid China and their significance for pollen-based quantitative climate reconstruction, Rev. Palaeobot. Palynol., 156, 519-524, https://doi.org/10.1016/j.revpalbo.2009.05.001, 2009.

Zhao, Y., Liu, H. Y., Li, F. R., Huang, X. Z., Sun, J. H., Zhao, W. W., Herzschuh, U., and Tang, Y.: Application and limitations of the *Artemisia*/Chenopodiaceae pollen ratio in arid and semi-arid China, Holocene, 22, 1385-1392, https://doi.org/10.1177/0959683612449762, 2012.

Zhao, Y. T., Miao, Y. F., Fang, Y. M., Li, Y., Lei, Y., Chen, X. M., Dong, W. M., and An, C. B.: Investigation of factors affecting surface pollen assemblages in the Balikun Basin, central Asia: Implications for palaeoenvironmental reconstructions, Ecol. Indic., 123, https://doi.org/10.1016/j.ecolind.2020.107332, 2021.

Zizka, A., Silvestro, D., Andermann, T., Azevedo, J., Ritter, C. D., Edler, D., Farooq, H., Herdean, A., Ariza, M., Scharn, R., Svantesson, S., Wengstrom, N., Zizka, V., and Antonelli, A.: CoordinateCleaner: Standardized cleaning of occurrence records from biological collection databases, Methods Ecol. Evol., 10, 744-751, https://doi.org/10.1111/2041-210X.13152, 2019.